Lappeenranta University of Technology
School of Energy Systems
Degree Program in Nuclear Energy Engineering

Ali Abdulnabi Alkhenaizi

STEAM GENERATOR DESIGNS FOR MODULAR PWR TEST REACTOR

Examiners : Professor D.Sc. Juhani Hyvärinen
D.Sc. Juhani Vihavainen

Supervisor: D.Sc. Juhani Vihavainen
Laboratory Engineer

ABSTRACT

Lappeenranta University of Technology
School of Energy Systems
Degree Program in Nuclear Energy Engineering

Ali Abdulnabi Alkhenaizi

Steam Generator designs for modular PWR test reactor

Master's Thesis

77 pages, 21 figures, 43 tables, 2 appendices

Examiners: Professor D.Sc. Juhani Hyvärinen
D.Sc. Juhani Vihavainen

Supervisor: D.Sc. Juhani Vihavainen

Keywords: PWR, VVER, Steam Generator, Experimental Test Facility, MOTEL, Scaling, EPR, AES-2006, NuScale, HT2S, Natural Circulation

The purpose of this Master's thesis is to scale-down the steam generator (SG) of three different PWR designs. The designs of concern were the vertical SG in the EPR, the horizontal SG in the AES-2006, and the helical SG in the NuScale reactor. The work contains a literature review for each PWR design, and their corresponding SG followed by the available scaling techniques. The scaling technique used in this work was the H2TS method and the focus of the scaling was on the 1-phase and 2-phase natural circulation. Based on the results from the scaling, a proposal was made for the three SG types which includes the size of the SG, operating pressure and temperatures, mass flow rates, tube sizes and layout, number of tubes, tube lengths, and tube diameters.

ACKNOWLEDGEMENTS

To begin with, I would like to express my sincere gratitude to my supervisor Dr. Juhani Vihavainen of the Nuclear Engineering department at Lappeenranta University of Technology (LUT) for his continuous guidance throughout the work of my thesis.

I would also like to thank Prof. Juhani Hyvärinen and the staff of Nuclear Engineering department at LUT for teaching me the basics of Nuclear Engineering during my Master's degree studies.

Last but not least, I wish to thank my parents and my family for their endless support and encouragement throughout my life. This accomplishment would not have been possible without them. Thank you.

May 2019
Ali Alkhenaizi

TABLE OF CONTENTS

LIST OF TABLES

LIST OF FIGURES

LIST OF SYMBOLS AND ABBREVIATIONS

AES	Atomnaya Elektrostantsiya (Nuclear Power Plant)
ADS	Automatic Depressurization System
APEX	Advanced Equipment Experiment
CMT	Core Makeup Tank
ECC	Emergency Core Cooling
ECCS	Emergency Core Cooling Systems
EPR	European Pressurized Reactor
EUR	European Utilities Requirements
FCM	Fractional Change Metric
FCSA	Fractional Change Scaling and Analysis method
FOM	Figure Of Merit
FRC	Fractional Rates of Change
FSA	Fractional Scaling Analysis
IAEA	International Atomic Energy Agency
IRWST	In-containment Refueling Water Storage Tank
I&C	Instrumentation and Control
H2TS	Hierarchical Two-Tiered Scaling
HCSG	Helical Coil Steam Generator
LB	Large Break
LCS	Lower Containment Sump
LOCA	Loss-Of-Coolant Accident
LUT	Lappeenranta University of Technology
LWR	Light Water Reactor
MOTEL	Modular Test Loop
NPM	NuScale Power Module
NPP	Nuclear Power Plant
NRSTH	Nuclear Reactor System Thermal hydraulics
PACTEL	Parallel Channel Test Loop
PWR	Pressurized Water Reactor
RCP	Reactor Circulation Pump
SB	Small Break

SG	Steam Generator
SMR	Small Modular Reactor
TMI-2	Three Mile Island Accident
TVO	Teollisuuden Voima Oyj
VTT	VTT Technical Research Centre of Finland
VVER	Voda-Vodyanoj Energeticheskij Reaktor (Water-Water Energetic Reactor)

LIST OF ANNOTATIONS

d_H	Hydraulic diameter
d_i	Hydraulic diameter of the *i*-th component
δ_i	Conduction depth
u_o	Reference velocity
ΔT_o	Temperature difference across the core
l_o	Equivalent length (heated length)
a_i	Cross-sectional flow area of the *i*-th component
a_{is}	Solid structure cross-sectional area of the *i*-th component
a_o	Cross-sectional flow area at the reference component
ξ_i	Wetted perimeter of the *i*-th component
α	Volumetric concentration
L	Spatial scale
τ	Temporal scale
ω_{CG}	Characteristic frequency of a specific process across an area A_{CG}
ω_i	Characteristic frequency in the control volume V_{CV}
ψ	Property (Mass, Momentum, Energy)
j_i	Property flux
Q_f	Volumetric flow rate
T_{cold}	Cold leg temperature in the primary side
T_{hot}	Hot leg temperature in the primary side
T_{sat}	Saturation temperature
P_{prim}	Nominal pressure in the primary side
Π_i	Characteristic time ratio
Π_{Ri}	Characteristic time ratio for 1-phase natural circulation
Π_h	Characteristic time ratio for 2-phase natural circulation
D	Scaling distortion
ρ	Density
β_T	Thermal expansion of primary side's fluid
g	Gravitational acceleration
H	Height or elevation

H_{pump}	Pump head
q_c	Quantity of heat generated from the core
F	Total loss coefficient
H_{TB}	Height of the tube bank
L_T	Tube length in the horizontal SG
F_{HGS}	Factor of characteristic pressure difference
f	Friction factor
K	Sum of form losses
Re	Reynold Number
μ	Kinematic viscosity
l_c	Axial length
a_c	Cross-section flow area
d_{tube}	Tube diameter
$\dot{m}$	Mass flow rate
α	Vapor volume fraction
u_{lo}	Velocity of the flow
u_f	Fluid velocity in the primary side
$\Delta\rho$	Density difference between the liquid phase and gas phase
C_p	Specific Heat
n_{tubes}	Number of tubes in the SG
n_{loops}	Number of loops in the primary side
p_{tri}	Triangular pitch
p_{rect}	Rectangular pitch
d_{tube}	Tube diameter
S_{tube}	Wall thickness of tube
a_{tube}	Cross-section area inside the tube
$d_{channel}$	Diameter of primary side's flow channel area for helical SG
d_{rod}	Control rod diameter in helical SG
d_{inner}	Diameter of the circle of the inner tube in the helical SG from the center of the tube from one side to center of tube on the other side
d_{outer}	Diameter of the circle of the outer tube in the helical SG from the center of the tube from one side to center of tube on the other side

1 INTRODUCTION

The objective of this section is to provide an introduction to Pressurized-Water Reactors (PWR) and Steam Generators (SG). The section covers how the PWRs works under normal operations and then focuses on the component of interest, the SG. Research method subsection covers the various available data from actual SG designs which are used in the next chapters to develop laboratory-scaled models.

1.1 Background

PWR is one of the most popular thermal reactors for electric power production. The origin of development for this type of reactor goes to nuclear driven submarines (Hewitt & Collier, 2000, p. 43). A schematic illustration of a simple PWR circuit is shown in Figure 1. The circuit consists of 3 independent closed cycles, those are: primary, secondary, and tertiary.

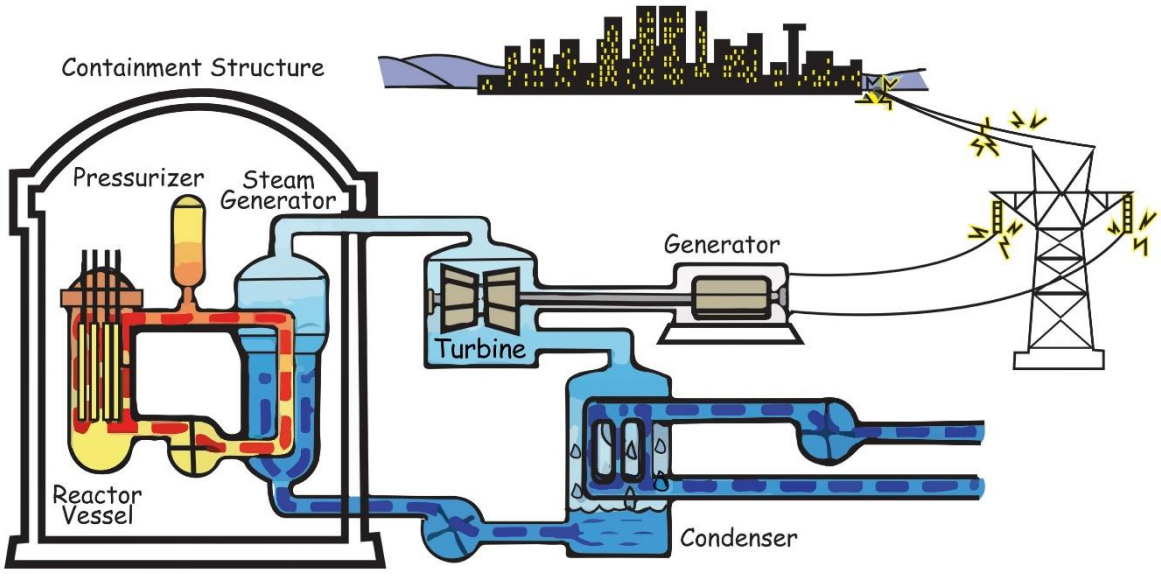

Figure 1 – Simplified schematic diagram of PWR showing its main loops (Nuclear Energy, 2018)

The heat source which is made from nuclear fuel rods is located inside the reactor vessel in the primary loop. The energy produced from the controlled fission reaction is released in the form of heat and modirated with circulating water as a coolant. Due to the pressure inside of the reactor vessel the coolant remains in liquid form and does not experience bulk boiling or vaporize. The heat carried by the coolant is transferred to the secondary loop when it is pumped through the steam generator tubes. The process continues and repeats itself as the coolant returns back to the reactor vessel. In order to maintain the pressure inside the vessel

to be above the saturation pressure to prevent bulk boiling, a pressurizer is connected to the primary loop. (Westinghouse Electric Corporation, 1984, p. 3)

Heat utilization occurs in the secondary loop. The hot coolant from the primary loop passes through the tubes of steam generator while water at lower pressure than the primary loop is injected inside the steam generator shell where it contacts the tubes outside surface. This process generates dry steam in the secondary loop. The steam then flows to the turbine and expands to convert its thermal energy into mechanical energy that rotates the turbine which then rotates the generator to produce electrical energy. The condenser after the turbine receives the expanded wet steam and the remaining latent heat of vaporization is transferred to the tertiary loop and condenses the steam into water. To continue the secondary loop cycle, the condensate is pumped back to the steam generator. (Westinghouse Electric Corporation, 1984, p. 3)

In the tertiary loop, the latent heat of vaporization gets discarded to the environment through the condenser cooling water. The tertiary loop could be either a once-through cooling loop where heat is released to surface water such as a lake, river, sea, or ocean, or the heat is rejected to the air (Westinghouse Electric Corporation, 1984, p. 4). The type of tertiary loop depends on the plant location. When no natural water body is available or available water quantity is insufficient then cooling towers are used. Another possibility to use cooling towers is when the water reservour could not accept the rejected heat due to the environmental aftermath (IAEA, 1974, p. 20).

A typical PWR plant in general has 3 or 4 independent primary loops, each of which with its own corresponding secondary and tertiary loops, per reactor pressure vessel (IAEA, 2007, p. 6). The advantage of having the primary loop separated from the secondary loop using a steam generator is that radioactive material in the primary loop is confined during normal power operation due to the absence of radioactively contaminated steam. As a result, extensive turbine maintenance problems are eliminated (Westinghouse Electric Corporation, 1984, p. 4). Additionally, PWRs tends to have smaller core size than that of other nuclear reactors because they have high volumetric power density as Table 1 shows (Hewitt & Collier, 2000, p. 46).

Table 1 – Core dimensions and thermal data for various reactor systems (Hewitt & Collier, 2000, p. 39)

Type	Reactor	Thermal Power (MW(t)	Core Diameter (m)	Core Height (m)	Core Volume (m^3)	Average Vol. Power Density (MW/m^3)	Average Fuel Rating (MW/tonne)	Average Linear Fuel Rating (kW/m)
Magnox	Calder Hall	225	9.45	6.40	449	0.50	—	—
	Bradwell	538	12.19	7.82	913	0.59	2.20	26.2
	Wylfa	1875	17.37	9.14	2166	0.865	3.15	33.0
AGR	Hinkley B	1500	9.1	8.3	540	2.78	11.0	16.9
	Hartlepool	1507	9.3	8.2	557	2.0	11.5	16.1
HWR	CANDU	3425	7.74	5.94	280	12.2	26.4	27.9
LWR	PWR	3800	3.6	3.81	40	95	38.8	17.5
	BWR	3800	5.01	3.81	75	51	24.6	19.0
RBMK	Chernobyl	3140	11.8	7.0	765	4.10	15.4	14.31
Fast	Phenix	563	1.39	0.85	1.38	406	149	27.0
reactor	PFR	612	1.47	0.91	1.61	380	153	27.0

There are 450 operating reactors of various types with over 1300 operational SGs as of January 2017. These reactors contribute with roughly 13.5% of total electricity power generated around the world. Such plants are reliable and an essential energy source that is technically free from “green-house” gases for electricity generation (Riznic, 2017, p. 15).

During the operation of a nuclear power plant, electricity generation is sustained through self-supporting fission chain reactions. For a safe operation of the power plant, such radioactivity and its fission products must be kept under control to avoid radioactive release to the environment. Therefore, fuel must be kept intact in all conceivable conditions. As a result, intentional malfunctions or accidents are avoided in actual operating reactors due to the high adverse consequences involved. Consequently, studying the effects of malfunctions and accidents are done theoretically and experimentally in experimental test facilities.

1.2 Experimental test facilities

An experimental test facility should not be confused with research reactors. A research reactor is a facility that provide a neutron source for research and various applications such as training and education, however, they are not used for power generation. Size wise, they are smaller than power generation reactors (IAEA, 2016, p. 2). As a result, their designed

power ratings go up to 10 MW thermal compared to 3000 MW thermal for a typical large power reactor unit (Tuunanen, et al., 1998, p. 8). Additionally, they tend to be simpler than power reactors, operates at lower temperatures, and requires inferior amount of fuel.

One example of a research reactor is FiR 1, which operated in Finland from 1962 until 2015. It is the first reactor in Finland to be decommissioned and lessons learned from Danish and German reactors decommissioning will be applied during the process. The timeline for FiR 1 research reactor can be found in Table 2. (VTT, 2015)

Table 2 – FiR 1 Research Reactor timeline (VTT, 2015)

Year	Status
Historical events	
1962	Helsinki University of Technology commissions a Triga Mark II research reactor, which is named FiR 1.
1967	The maximum thermal power is raised to 250 kW following tests and modifications.
1971	The research reactor operational responsibility is moved from Helsinki University of Technology to VTT Technical Research Centre of Finland.
1999	The reactor is used for the first time to provide cancer treatment in collaboration with the Hospital District of Helsinki and Uusimaa.
2012	The cancer treatment provider goes out of business.
2015	The reactor is run for the last time on 30 June 2015.
Future plans	
2019	The spent nuclear fuel is transported to the US or interim storage.
2019	The reactor is dismantled, and the resulting waste placed in interim storage.
2022	The empty reactor building is decontaminated and released.
2030	The waste is transported from the interim storage facility to a final repository.

On the other hand, an experimental test facility is a scaled-down facility from a reference reactor. The components of the facility do not include an actual core, neither fissile fuel, and instead are replaced with heating elements to simulate the heat generated from nuclear fission. A test facility ranges from being a simple set-up to a fully integrated model for the

whole primary circuit. The main purpose of such a facility is to study thermal hydraulics and the behavior of light water reactors (LWR). (Kouhia, et al., 2014, p. 6)

Experimental thermal hydraulic studies were conducted in Lappeenranta University of Technology (LUT) since 1975 (Kouhia, et al., 2014, p. 6). Various facilities have been built since and PACTEL is one of them. The reference reactor for PACTEL is the PWR reactor VVER-440 which is operating in Loviisa, Finland. Major components and systems of the reference PWR are simulated in PACTEL facility during assumed loss-of-coolant accidents (LOCA) and operational transients. The primary system, the secondary side of the steam generators, and the emergency core cooling systems (ECCS) all are included in the PACTEL facility. A comparison of the main characteristics of the PACTEL facility with its reference reactor VVER-440 reactor are shown in Table 3 and a general view of the PACTEL facility is shown in Figure 2. (Tuunanen, et al., 1998, p. 10)

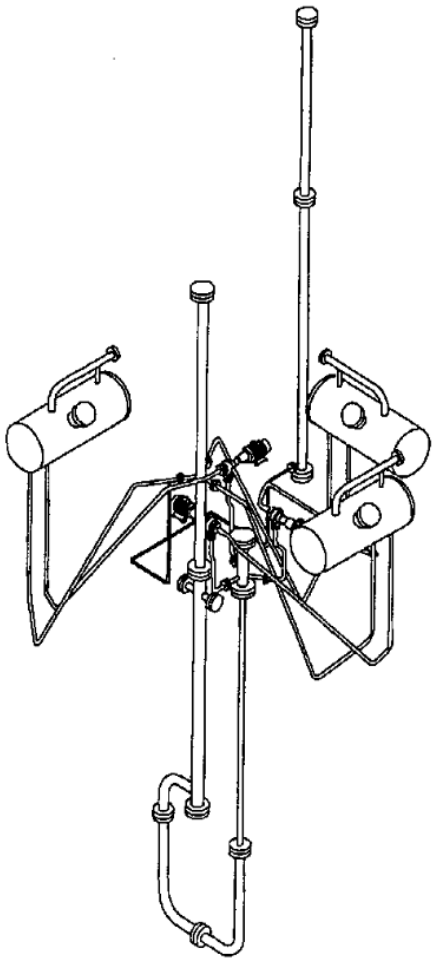

Figure 2 – The PACTEL facility (Tuunanen, et al., 1998, p. 12)

Table 3 – PACTEL facility characteristics compared with VVER-440 reactor (Tuunanen, et al., 1998, p. 11)

Characteristic	**PACTEL**	**VVER-440**
Reference power plant	VVER-440	-
Volumetric scaling ratio	1:305	-
Scaling factor of component heights and elevations	1:1	-
Number of primary loops	3	6
SG orientation (type)	Horizontal	Horizontal
Maximum thermal power (heating power)	1 MW	1375 MW
Number of rods	144	39438
Outer diameter of fuel rod simulators	9.1 mm	9.1 mm
Heated length of fuel rod simulators	2.42 mm	2.42 mm
Axial power distribution	Chopped cosine	Cosine
Axial peaking factor	1.4	1.4
Maximum cladding temperature	800 ℃	N/A
Maximum operating pressure	8.0 MPa	12.3 MPa
Maximum operating temperature	300 ℃	300 ℃
Maximum secondary pressure	5.0 MPa	5.0 MPa
Maximum secondary temperature	260 ℃	260 ℃
Feedwater tank pressure	2.5 MPa	2.5 MPa
Feedwater tank temperature	225 ℃	225 ℃
Accumulator pressure	5.5 MPa	5.5 MPa
Low-pressure ECC-water pressure	0.7 MPa	0.7 MPa
High-pressure ECC-water pressure	8.0 MPa	8.0 MPa
ECC-water temperature	30 ~ 50 ℃	30 ~ 50 ℃

The construction of European Pressurized Reactor (EPR) in Olkiluoto in Finland intensified the national research activities to the western type PWRs. Hence, the original PACTEL facility got modified into PWR PACTEL test facility utilizing some parts of the original facility such as the pressurizer, pressure vessel parts, and ECCSs. The fundamental difference between both facilities is in the loop and SG design. The original PACTEL design has three loops with horizontal SGs, whereas the PWR PACTEL consists of two loops with

a vertical SG in each. The PWR PACTEL facility characteristics are shown in Table 4 and a general view of the facility is shown in Figure 3**.** (Kouhia, et al., 2014, pp. 6-7)

Table 4 – PWR PACTEL facility characteristics (Kouhia, et al., 2014, p. 9)

Characteristic	**PWR PACTEL**
Reference power plant (loops and steam generators	PWR (EPR)
Volumetric scale: Pressure vessel, SGs, pressurizer	1:405, 1:400, 1:562
Height scale: Pressure vessel, SGs, pressurizer	1:1, 1:4, 1:1.6
Number of primary loops	2
SG orientation (type)	Vertical
Maximum core heating power	1 MW
Number of fuel rod simulators	144
Outer diameter of fuel rod simulators	9.1 mm
Heating length of fuel rod simulators	2.42 mm
Axial power distribution of the core section	Chopped cosine
Axial peaking factor of the core section	1.4
Maximum fuel rod simulator cladding temperature	750 ℃
Maximum design primary / secondary pressure	8.0 MPa / 4.65 MPa
Maximum design primary / secondary temperature	300 ℃ / 260 ℃
SG heat exchange tube diameter / thickness	19.05 mm / 1.24 mm
Average SG heat exchange tube length	6.5 m
Number of heat exchange tubes in SG	51
Number of instrumented heat exchange tubes in SG1 / SG2	8 / 51
Maximum secondary side feed water mass flow	30 l/min
Maximum feedwater tank pressure	2.5 MPa
Maximum accumulator pressure	5.5 MPa
Maximum HPIS / LPIS water pressure	8.0 MPa / 0.7 MPa
Main material of components	Stainless steel (AISI 304)
Insulation material	Mineral wool
Cover material	Aluminum

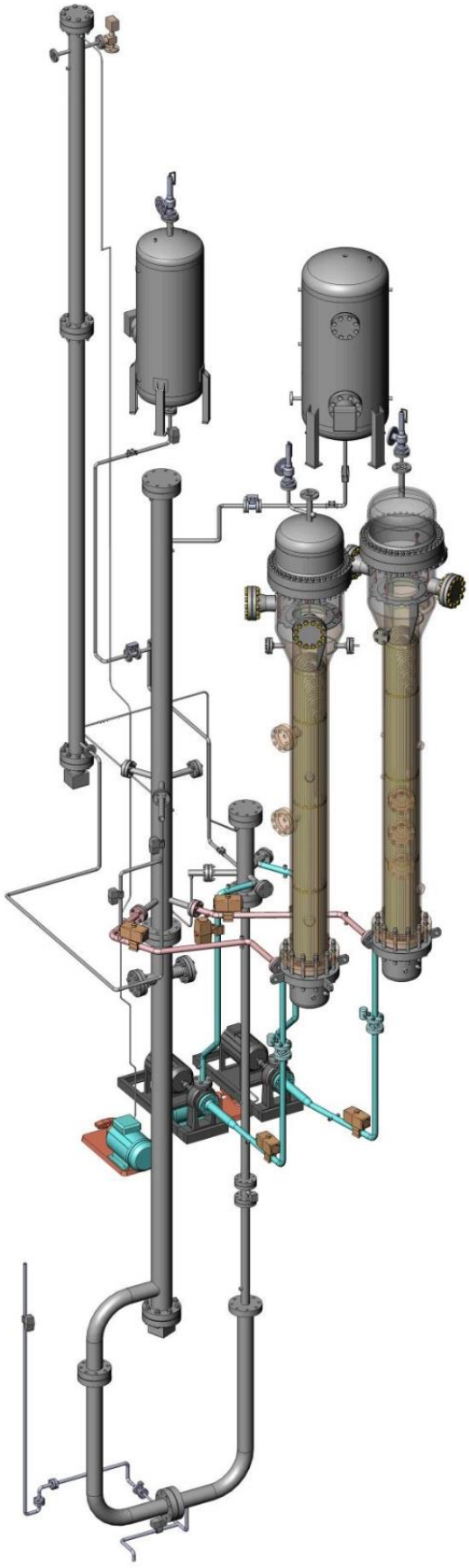

Figure 3 – The PWR PACTEL facility (Kouhia, et al., 2014, p. 8)

1.3 Research method

The main purpose of this thesis is to design scaled-down SGs and calculate the distortions which are caused due to the scaling. The designs will be based on specific reference plant SGs. The SG designs of concern are listed below with their corresponding nuclear power plant (NPP) type:

- Vertical SG design: EPR
- Horizontal SG design: VVER-1200, also called AES-2006
- Helical coil SG design: NuScale reactor

Each reactor type will be investigated to find out the concept behind its SG and extract the relevant data from the design. The next step is to introduce the scaling principle and scaling methodologies then choose a methodology to scale-down each SG design. The scaled-down model of each SG would include the number of tubes, tube size, tube length, diameters and the tube bundle geometry. These scaled-down parameters would represent the SG designs in a scale suitable for a Modular Test Loop (MOTEL) which LUT university is building (Hyvärinen, et al., 2017). The SG dryers will be excluded from the designs because the generated steam from the SGs would not be used to generate electricity and will be dumped into the air, therefore drying the steam would be redundant.

1.4 Structure of the thesis

This thesis work consists of six sections including the introduction. Section 2 consists of the NPP concepts for different SG types. Section 3 consists of scaling methods and the technique that is used in section 4 to obtain a model for the SG designs. Section 5 consists of the discussion of the findings from the scaling. Section 6 consists of a summarization of this work.

2 STEAM GENERATORS DESIGN CONCEPTS

This section focuses on the different designs of currently operating SGs which are used as references for the models for scaling-down technique. As the design of a SG changes, their features and operational performance indicators becomes unique. Table 5 displays statistical information for SGs by reactor type. The dominant reactor type both operational and under construction is the PWR as the same table shows. (Riznic, 2017, p. 16)

Table 5 – IAEA information on steam generators by reactor type, as of January 2017 (Riznic, 2017, p. 17)

Reactor type	**Number of operational**		**Number of under construction**		**SG tube materials**
	NPPs	**SGs**	**NPPs**	**SGs**	
PWR	233	705	36	113	Incoloy-800, Inconel-60, Inconel-600
VVER	57	274	15	64	Austenitic Stainless Steel (08CH18N10 T SS)
Once-through SG	6	12	0	0	Inconel-600, Incoloy-800
Heavy-water reactor	49	290	4	16	Incoloy-800, Inconel-600, Monel-400
Fast breeder reactor	3	5	1	2	ICR2MO
Light-water graphite reactor	15	68 (steam drums)	0	0	N/A
Gas-cooled reactor	14	76	0	0	BS3059/3 mild steel/9%CrMo steel/TP316 stainless steel, mild/chrome/ST, austenitic stainless steel & Cr/Mo, mild steel

2.1 European Pressurized Reactor (EPR)

The EPR is a revolutionary 1600 MW electric PWR design based on experience from several reactor years of operation globally, primarily those incorporating the most recent technologies such as the Konvoi and N4 reactors operating in Germany and France respectively. Table 6 provides a list of the commissioned Konvoi and N4 reactors. Major innovations are featured in the EPR especially in further prevention of core meltdown and relieve its potential consequences. Furthermore, the EPR design avail from outstanding resistance to external hazards, including air-plane crash and earthquake. The operating and safety systems in the EPR contributes in progressive responses proportional with any abnormal occurrences. (Areva, 2005, p. 2)

Table 6 – List of Konvoi and N4 NPP constructed in Germany and France respectively (TVO, 2010, p. 4)

Reactor	Rated electric power	Commission year
Germany (Konvoi reactors)		
Neckarwestheim 2	1269 MW	1989
Isar 2	1400 MW	1988
Emsland	1290 MW	1988
France (N4 reactors)		
Chooz 1	1450 MW	1996
Chooz 2	1450 MW	1997
Civaux 1	1450 MW	1997
Civaux 2	1450 MW	1999

In terms of technological advances, the EPR is at the forefront of NPP design. The main features of the design include:

- Flexibility of fuel management for the reactor core.
- The reactor protection system.
- The instrumentation and Control (I&C) system, the operator friendly man-machine interface and fully computerized control room of the plant.
- The large components such as the reactor pressure vessel and its internal structures, steam generators and primary coolant pumps.

The innovative design offered by the EPR contribute to the high level of performance, efficiency, operability and therefore economic competitiveness to fully satisfy the expectations of customers for their future NPPs. (Areva, 2005, p. 2)

The first customer to sign a contract to build an EPR was the Finnish electricity utility Teollisuuden Voima Oyj (TVO). The contract was signed on 18th December 2003 and the scheduled commercial operation was in 2009.(Areva, 2005, p. 59). However, the start of the NPP was delayed until May 2019 (Reuters, 2017) and TVO had a settlement with the construction company by a financial compensation of 450 million Euros (TVO, 2018). The construction of the plant, namely Olkiluoto 3, is a consortium formed by Areva and Siemens. Areva is responsible to deliver the reactor plant (primary side) while Siemens is delivering the turbine plant (secondary side) (TVO, 2010, p. 4). A schematic diagram of Olkiluoto 3 showing its principal safety features is shown in Figure 4.

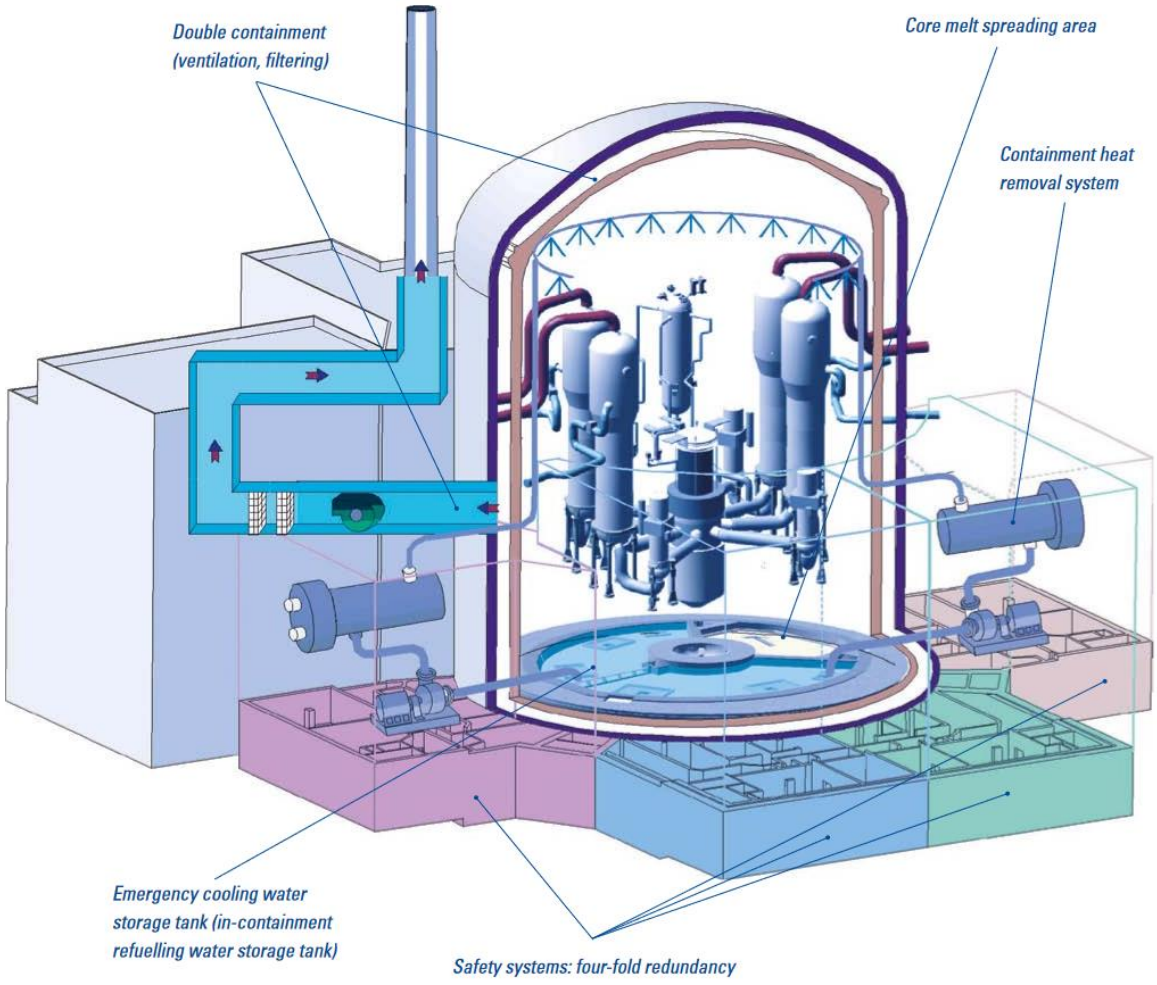

Figure 4 – Schematic diagram of Olkiluoto 3 showing its principle safety features (TVO, 2010, p. 42)

The interface between the water in the primary loop and secondary loop is the SGs which provides steam to the turbine generator. Water from the primary loop flows inside the SG tube bundle and transfers heat to water in the secondary loop to produce steam. The SG in

EPR is an improved version of the N4 steam generator. It is a vertical, U-tube, natural circulation heat exchanger equipped with an axial economizer. The axial economizer increases the steam pressure output by 3 bars compared to a conventional design. This increase in the saturation pressure of the steam makes it possible for the plant to reach an efficiency of 36 to 37% depending on the site. Additionally, the axial economizer does not obstruct access to the tube bundle for inspection and maintenance. (Areva, 2005, p. 26)

The design of the SG is composed of two subassemblies, those are: the one insuring vaporization of the secondary feedwater (U-tube bundle), and the mechanically drying the steam-water mixture produced assembly (steam drier) (Areva, 2005, p. 26). A schematic diagram for the EPR steam generator of Olkiluoto 3 is shown in Figure 5.

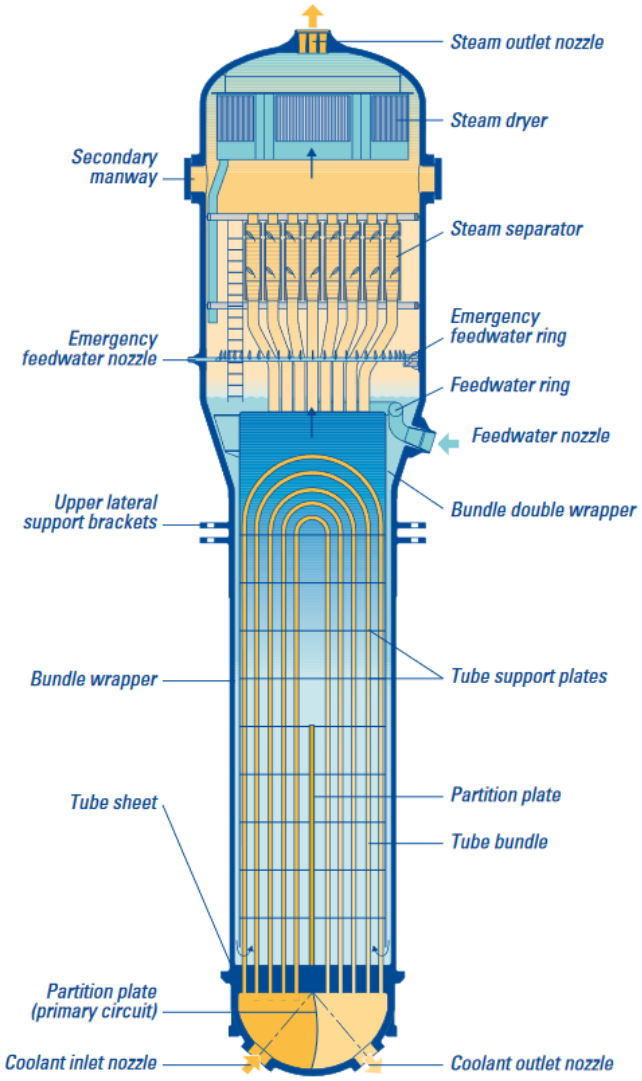

Figure 5 – Cutaway of steam generator in Olkiluoto 3 EPR showing its main components (TVO, 2010, p. 24)

The tube bundle in the EPR is protected against vibration using anti-vibration bars located at the U-section of the bundles. Furthermore, the SG is designed to cancel out secondary cross-flows which protects the tube bundle against vibration risks. (Areva, 2005, p. 26)

In the event of a total loss of feedwater, the mass of water on the secondary side has been increased to get a dry-out time in the SG of at least 30 minutes in the event of a total loss of feedwater (Areva, 2005, p. 26). Table 7 contains detailed properties for the EPR SG of Olkiluoto 3.

Table 7 – Steam generator properties for Olkiluoto 3 EPR (TVO, 2010, p. 24)

Characteristic	**Data**
Steam Generators	
Number of steam generators	4 units
Orientation of the steam generators	Vertical
Heat transfer surface per steam generator	7960 m^2
Primary circuit operating pressure	155 bars
Primary circuit inlet temperature	296 ℃
Primary circuit outlet temperature	329 ℃
Secondary circuit steam pressure	78 bars
Secondary circuit steam temperature	293 ℃
Tube outer diameter / wall thickness	19.05 mm / 1.09 mm
Number of tubes	5980 tubes
Triangular pitch of tubes	27.43 mm
Total height	15 m
Vessel diameter (outer)	3 m
Materials	
Tubes	Inconel 690 alloy, heat treated
Vessel	18 MND 5 (low-alloy ferrite steel)
Cladding tube sheet	Ni-Cr-Fe alloy
Tube support plates	13% Cr-treated stainless steel
Miscellaneous	
Rated power thermal/electric	4300 / 1600 MW
Total mass	520 tons
Feedwater temperature	230 ℃
Main steam moisture content	0.25%
Main steam flow rate at nominal conditions	2443 kg/s

2.2 AES-2006

The AES-2006 is a generation 3+ reactor developed in Russia that is also referred to as VVER-1200 (Rosatom Overseas JSC, 2015, p. 13). The terms AES and VVER are translated from Nuclear Power Plant and Water-Water Energetic Reactors respectively. In 1964, the first VVER unit was commissioned at Novovoronezh nuclear power plant in Russia. Testing ground for new VVER began since that time at Novovoronezh nuclear power plant (Rosatom Overseas JSC, 2015, p. 8). Today, Russia became a leading nuclear constructor abroad and the first place in terms of construction projects is held by Rosatom (Rosatom, 2018). Table 8 presents the VVER generations and the countries operating them.

Table 8 – VVER Generations (Rosatom Overseas JSC, 2015, p. 13)

GEN I VVER	GEN II VVER-440	GEN II/GEN III VVER-1000	GEN III+ VVER-1200
V-210 **RUSSIA:** Novovoronezh 1 *(decommissioned)* V-365 **RUSSIA:** Novovoronezh 2 *(decommissioned)*	V-179 **RUSSIA:** Novovoronezh 3-4 V-230 **RUSSIA:** Kola 1-2 *Decommissioned:* **EAST GERMANY:** Greifswald 1-4 **BULGARIA:** Kozloduy 1-4 **SLOVAKIA:** Bohunice I 1-2 V-213 **RUSSIA:** Kola 3-4 **UKRAINE:** Rovno 1-2 **HUNGARY:** Paks 1-4 **CZECH REP.:** Dukovany 1-4 **FINLAND:** Loviisa 1-2 **SLOVAKIA:** Bohunice II 1-2 Mochovce 1-2 Mochovce 3-4 *(under construction)* V-270 **ARMENIA:** Armenia-1 *(decommissioned)* Armenia-2	V-187 **RUSSIA:** Novovoronezh 5 V-302 **UKRAINE:** South Ukraine 1 V-338 **UKRAINE:** South Ukraine 2 **RUSSIA:** Kalinin 1-2 V-320 **RUSSIA:** Balakovo 1-4, Kalinin 3-4, Rostov 1-2, Rostov 3-4 *(under construction)* **UKRAINE:** Rovno 3-4, Zaporozhe 1-6, Khmelnitski 1-2, South Ukraine 3 **BULGARIA:** Kozloduy 5-6 **CZECH REP.:** Temelin 1-2 V-428 **CHINA:** Tianwan 1-2, Tianwan 3-4 *(under construction)* V-412 **INDIA:** Kudankulam 1 , Kudankulam 2 *(under construction)* V-466 **IRAN:** Bushehr 1	V-392M **RUSSIA:** Novovoronezh II 1-2 *(under construction)* V-491 **RUSSIA:** Baltic 1-2 *(under construction)* Leningrad II 1-2 *(under construction)* **BELARUS:** Belarus 1 *(under construction)*
1960	1970	1980	1990	2000	2010

The development of AES-2006 design was a collaboration between Organization of General Designer (Atomenergoproekt), Organization of General Designer of reactor plant, OKB Gidropress, with the scientific supervision of the RRC (Kurchatov Institute). The design is in compliance with the Russian Regulatory Documents, the IAEA requirements, and the European Utilities Requirements (EUR). Furthermore, an accumulated 1400 reactor-years

of operation and decommissioning of VVER reactors experience endorsed the engineering solutions found in those reactors (IAEA, 2011, p. 2). Specific features of the AES-2006 design are listed below and a schematic of the plant is shown in Figure 6.

- The main irreplaceable equipment of the reactor plant's service life is 60 years.
- Horizontal SG layout with a large water inventory and improved natural circulation conditions of the primary-side compared to vertical SG layout.
- Active and passive operation principles for ECCS.
- Double envelope concrete containment.
- Improved I&C reliability with self-diagnostics function.
- Reactor pressure vessel with minimum number of welds. The vessel is manufactured by forged shells without longitudinal welds, which reduces inspection time.
- Reactor vessel has no incuts and/or holes below the reactor main nozzles.
- During loss of power, the Reactor Circulation Pumps (RCP) are designed to provide the required decrease in the flow rate through the core.

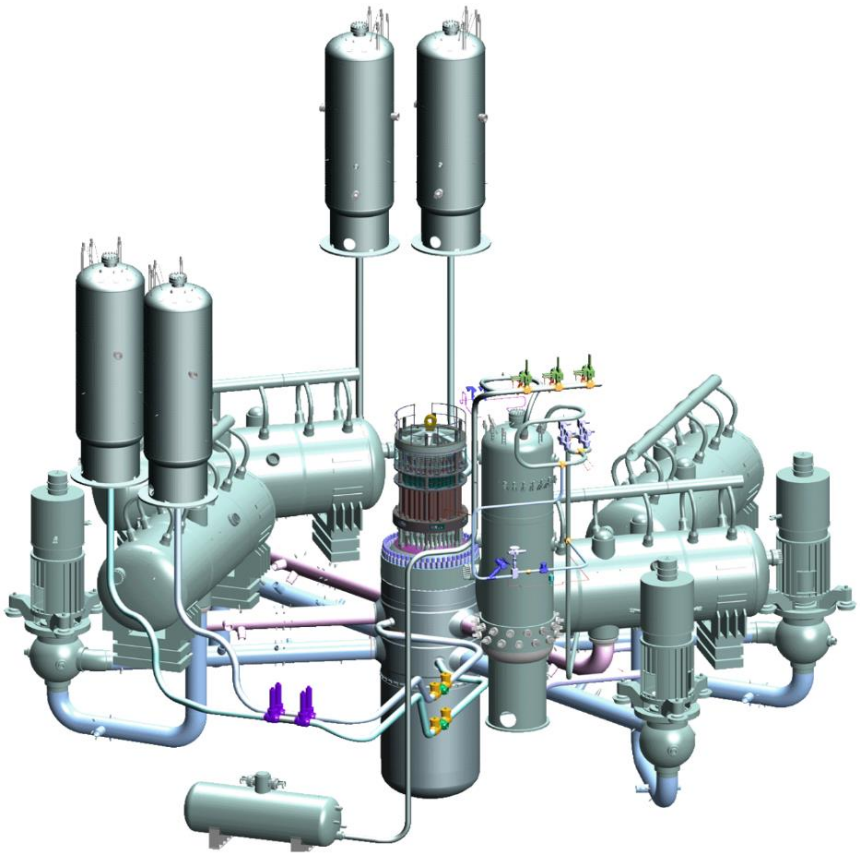

Figure 6 – Main components of the AES-2006 reactor (Rosatom Overseas JSC, 2015, p. 26)

The main features of VVERs including the AES-2006 are the hexagonal fuel assembly and horizontal SG layout. Due to the horizontal layout, the SGs do not experience problems such as primary water stress-corrosion cracking, denting and fouling. Historical data shows for more than 35 years several VVER-440 plants operated without corrosion of SG heat exchanger tubes that required tube plugging. (Rosatom Overseas JSC, 2015, p. 29)

The AES-2006 operates with PGV-1000MKP type SGs. In addition to the horizontal layout, the heat-exchanger tubes in the tube bundle uses a "corridor" layout. The final design which includes efficient sludge removal from the SG bottom, the utilization of secondary side ethanolamine water chemistry, and removal of copper-bearing components on the secondary side, provided an expected 60 years of achievable service life (Rosatom Overseas JSC, 2015, pp. 29-30). Table 9 contains detailed properties for the PGV-1000MKP type SG.

Table 9 – Properties for PGV-1000MKP type steam generator (IAEA, 2011, pp. 6-7, 29-30)

Characteristic	**Data**
Steam Generators	
Number of steam generators	4 units
Orientation of the steam generators	Horizontal
Heat transfer surface per steam generator	6105 m^2
Primary circuit operating pressure	162 bars
Primary circuit inlet temperature	298.2 ℃
Primary circuit outlet temperature	328.9 ℃
Secondary circuit steam pressure	68 bars
Secondary circuit steam temperature	283.8 ℃
Tube outer diameter / wall thickness	16.0 mm / 1.5 mm
Number of tubes	10978 tubes
Square pitch of tubes (vertical / horizontal)	22 mm / 24 mm
Vessel length / diameter	13.82 m / 4.2 m
Materials	
Tubes	08H18N10T stainless steel
Vessel	10GN2MFA steel
Miscellaneous	
Rated power thermal / electric	3200 / 1200 MW
Total mass	330 tons
Feedwater temperature	227 ℃
Feedwater flow rate at nominal conditions	1780 kg/s

Saturated steam produced in the SG flows through holes in a perforated sheet immersed below the evaporation surface. In the vapor space steam is dried via gravitation and flows to a perforated distribution sheet located at the upper part of the SG. After that, the steam enters the steam header through 10 nozzles. The perforated sheets long the length of the SG is where steam production rate equalization takes place. (Rosatom Overseas JSC, 2015, p. 30)

Free of moisture steam flows out of the steam header into the steam lines. The feed water flows through pipework into the SG's feedwater distribution header. In the event of emergency cooldown, an emergency feed water system provides the feed water supply. Water in the secondary side of the SG circulates naturally. The heat transfer surface of the SG consists of stainless steel tubes with a highly firm support structure in comparison with those used in vertical PWR SGs. Figure 7 shows a schematic diagram of PVG-1000MKP type horizontal SG used in AES-2006 reactors.

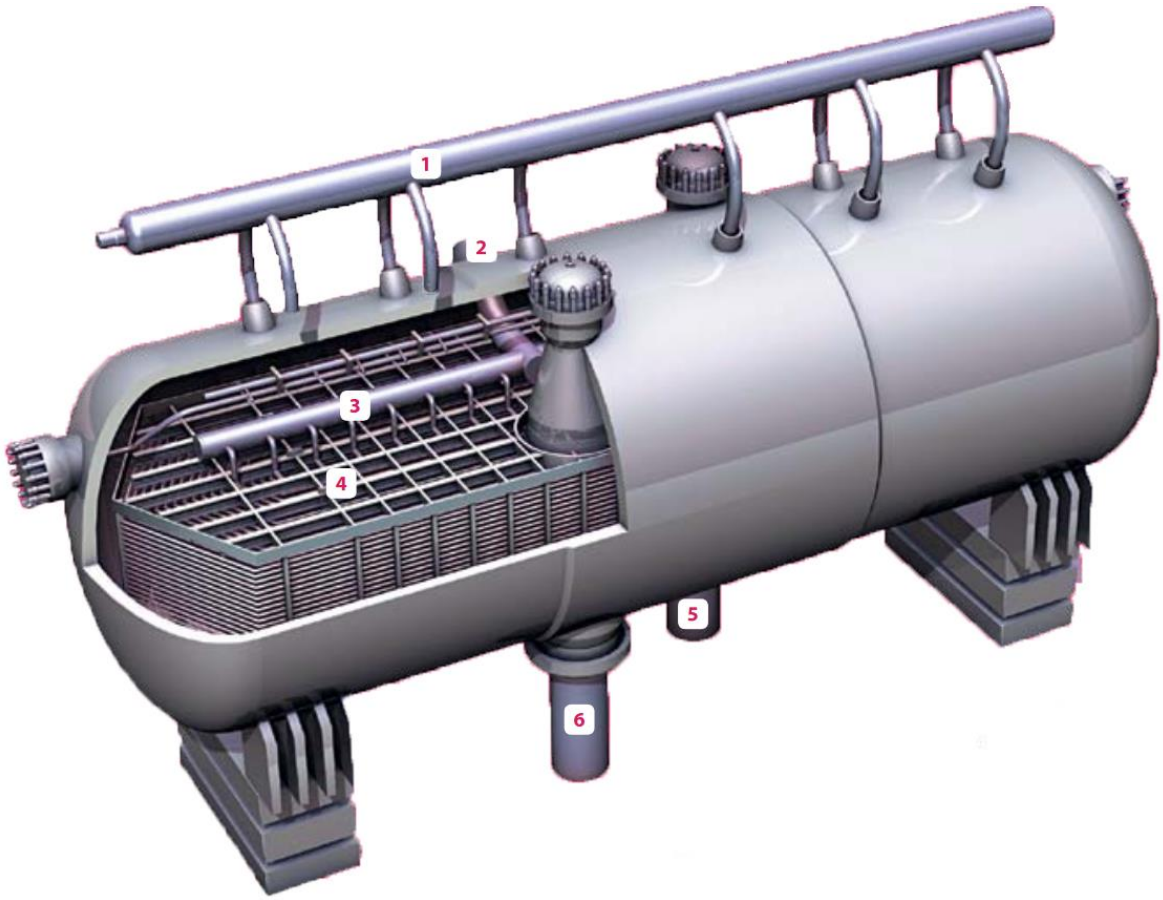

Figure 7 – PGV-1000MKP type steam generator. Numbers in the figure are: 1. Steam header, 2. Feedwater inlet, 3. Feedwater header, 4. Heat exchange tubes, 5. Main coolant inlet, 6. Main coolant outlet (Rosatom Overseas JSC, 2015, p. 29)

2.3 NuScale Power Module (NPM)

The idea behind Water-cooled Small Modular Reactors (SMR) concept was developed as a response to the challenges in the 21st century (Reyes, 2009, p. 3). Various global companies developed programs for small (less than 300 MWe) and Medium (between 300 and 700 MWe) water-cooled reactors (Reyes, 2009, pp. 3-4) (IAEA, 2014). One of these design projects were funded by the United States Department of Energy and NuScale Power company was founded as a result (Modro, et al., 2003, p. ii) (Bergman, et al., 2016, p. 5).

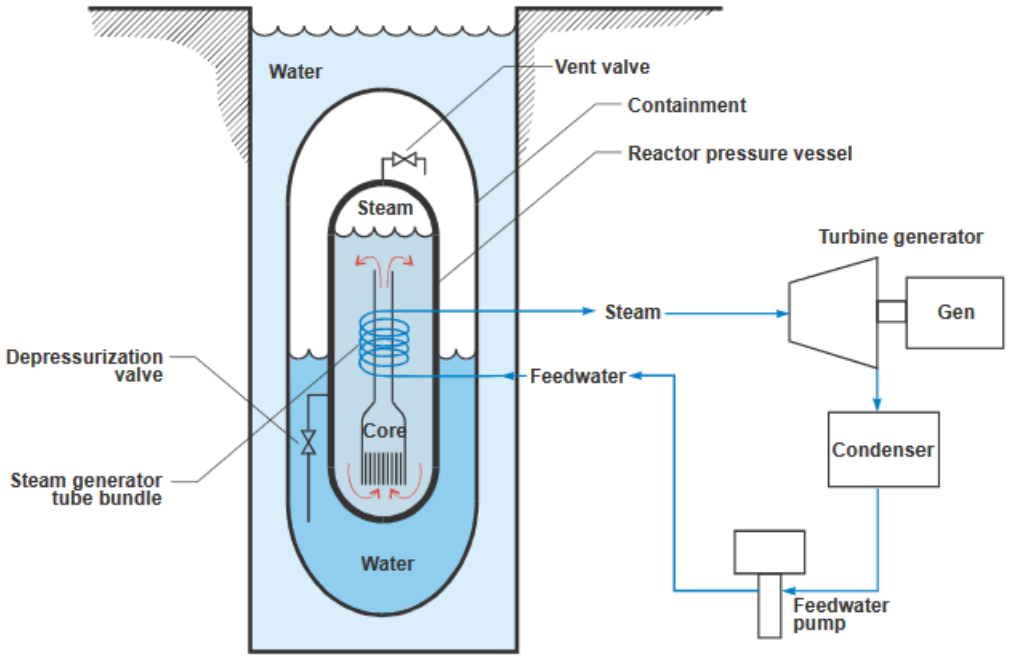

Figure 8 – SMR Design concept for NuScale reactor (Modro, et al., 2003, p. iii)

The main aim of the project was to develop a modular reactor design which is composed of a self-contained assembly that has the reactor vessel, SGs, and the containment. The module would have the feature of being manufactured as single units then shipped individually to finally be assembled in a rector building. The concept of the project is shown in Figure 8 which has the following unique features (Modro, et al., 2003, pp. ii-iii):

- The primary vessel contains the reactor core and the SG tube bundles. This eliminates the need of piping to connect the SG with the reactor.
- The absence of rotating equipment in the primary system due to primary coolant flow because of buoyancy forces.

- The reactor vessel and its steel containment are immersed in water enabling an effective passive ultimate heat sink.
- Refueling and maintenance is done every 5 years and a refurbished module instantly is used as a replacement. The module is removed and mobilized while being under water.

After years of development, the NuScale Power Module (NPM) was created. The NPM consists of an integrated reactor core, two helical coil steam generators (HCSG), and a pressurizer inside a pressurized reactor vessel that is installed within a compact steel containment vessel. Furthermore, the design provides the ability to use from 1 and up to 12 NPM units for one reactor building. (NuScale Power, 2018, p. 8)

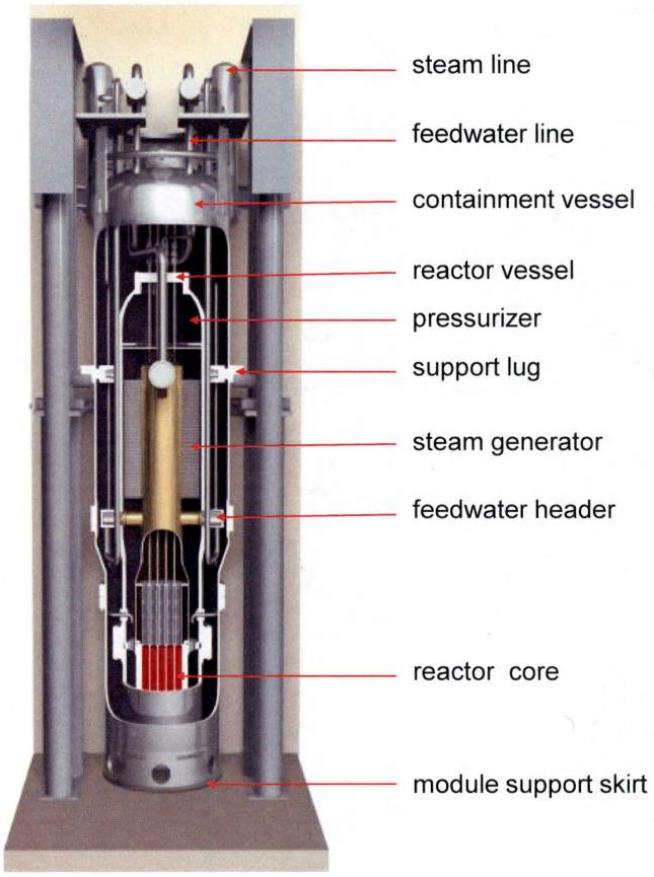

Figure 9 – Sectional view for an NPM showing its internal components (Bergman, et al., 2016, p. 23)

Each single NuScale module unit does not require AC or DC power for safe shut down and cooling. The core of the unit is relatively small hence the potential radiation source term in an accident is small. The containment of the unit is made of high-strength steel and during

normal operation it is sub-atmospheric pressurized while immersed in a pool of water. The feature of interest from the module is its compact HCSGs with pressurized tubes from the outside (NuScale Power, 2018, p. 8). A schematic cross-section of the NuScale reactor is shown in Figure 9.

Steam production in the NPM uses 2 once-through helical coil SGs. The space between the hot leg riser and the reactor vessel hosts the SGs. Each SG is made of tubes connected to feed and steam plenums with tube sheets. Nozzles on the reactor vessel provides an entrance for the preheated feedwater. Heat is transferred from the reactor coolant to the feedwater across the SG tube wall as the feedwater flows inside the SG tubes. The phase of the feedwater changes into a superheated steam as it passes through the SG (NuScale Power, 2018, p. 29). The number of SG tubes and other characterizes of the SG can be found in Table 10.

Table 10 – NuScale SG specifications (NuScale Power, 2018, p. 12) (NuScale Power, 2018, p. 46) (NuScale Power, 2018, p. 80) (Bergman, et al., 2016, p. 29)

Characteristic	**Data**
Steam Generators	
Number of steam generators	2 units
Orientation of the steam generators	Vertical helical tube
Heat transfer surface area (total)	1672.25 m^2
Primary circuit operating pressure	127.5 bars
Primary circuit inlet temperature	258.3 ℃
Primary circuit outlet temperature	283.8 ℃
Secondary circuit operating pressure	34.5 bars
Live steam temperature	301.67 ℃ / 57 of superheat
Tube outer diameter / wall thickness	N/A
Number of tubes (total)	1380 tubes
Vessel height / inner diameter	23.07 m / 4.32 m
Materials	
Tubes	N/A
Vessel	Stainless steel
Miscellaneous	
Rated power thermal / electric	160 / 50 MW
Total mass	762 tons
Feedwater temperature	204 ℃
Live steam flow rate	67.04 kg/s

3 SCALING METHODOLOGY

One of the main foundations for the safety and design technology of water-cooled reactors is Nuclear Reactor System Thermal hydraulic (NRSTH). The nominal operating conditions of water cooled reactors are associated with high pressure, high thermal power, high power density, and large two-phase volume mixture. Since it is hazardous to perform meaningful experiments related to accidental scenarios in an actual nuclear facility, a substitute would be required for these experiments. If the substitute in question would be made in full scale it would become impossible to conduct the experiments in it. Therefore, nuclear reactors performance simulations would be more feasible to be done and proven at reduced scale. (D'Auria & Galassi, 2010, pp. 2-3)

Another consideration for building a test facility is making it feasible to be built and scaling essentially provides cost reduction for the test facility. Due to the scaling process, the geometry of the test facility shrinks and the operating parameters gets reduced. Thus, there must be a rationale to dimension the test facility, design the tests, and interpret the results. In this section scaling technique is defined and followed by some examples of techniques used in thermal hydraulics.

3.1 Scaling techniques

The reduced scaled is obtained through a process called scaling. Scaling then can be defined as the methods, actions, and techniques that are used for the purpose of connecting the parameters related to experiments with conditions in actual NPPs. The process of scaling demonstrates the suitability of a parameter to reactor conditions (D'Auria, 2017, p. 115). However, a properly scaled facility that provides beneficial data from experiments would still suffer from “scaling distortions” as it would be impossible to satisfy all the scaling requirements (Ishii, et al., 1998, p. 209).

Various scaling analysis methodologies and techniques were developed since the 1960s (D'Auria & Galassi, 2010, p. 8). Power-to-volume scaling is an early method used for scaling and design of experimental facilities. In terms of scaling analysis and experimental data extrapolation, the most common methodologies are the three-level scaling by Ishii (Ishii, et al., 1998), Hierarchical Two-Tiered Scaling (H2TS) (Zuber, et al., 1998) and Fractional

Change Scaling and Analysis method (FCSA) (Zuber, 2001) by Dr Zuber. Each method is depicted in its own segment, focusing on the H2TS method as it is the method of choice to use to scaling down the SGs (D'Auria, 2017, p. 115).

3.1.1 Power-to-volume scaling

Prior to Three Mile Island accident (TMI-2), experimental facilities simulations were carried out focusing on Large Break LOCA (LB-LOCA). After the accident, the main focus of NRSTH research shifted to Small Break LOCA (SB-LOCA). During that time in history, the power-to-volume scaling approach was the preferred method for scaling of test facilities. (D'Auria & Galassi, 2010, p. 9)

The power-to-volume scaling method was introduced in 1979 which was the same year the TMI-2 occurred (D'Auria & Galassi, 2010, p. 9). In this method, the time, height, velocity, and heat flux of the prototype are equivalently conserved with the scaled-down model. The scaled-down model keeps its full-height scale ($l_R = 1$). The area and volume on the other hand are both reduced with the same scale ($a_R = V_R = {D_R}^2$). One advantage of this method is the preservation of gravity effect enabling the simulation of phenomena where the effect of gravity is important. Consequently, it is capable to simulate accidents in which flashing occurs by pressure decrease. Additionally, it can be used for heat transfer test in an electric heater bundle as nuclear fuel simulation, and critical heat flux test (Nuclear Energy Agency, 2017, p. 88).

On the other hand, applying the power-to-volume scaling to a test facility with significantly small area scale could distort major phenomena drastically. This is more apparent in pressure drop and heat losses of the system. Also, the heat accumulated in the structure of test facility become excessive for small scales. Furthermore, the area reduction due to full-height conservation increases the aspect ratio and therefore the simulation of multidimensional flow phenomena in the test facility becomes inadequate. (Nuclear Energy Agency, 2017, p. 88)

3.1.2 Ishii three-level scaling

In 1983 the three-level scaling method was introduced by Ishii & Kataoka which focuses on the conservation of natural circulation as it is widespread in accidents based on design. This

scaling method has the advantage of using different height and area ratios, enabling the design of test facilities with reduced height. (Nuclear Energy Agency, 2017, p. 91)

As the name of the method implies, it consists of three steps. The first step is the integral analysis to conserve the natural circulation flow in single-phase and two-phase (Ishii, et al., 1998, p. 180). The non-dimensional governing equations form of natural-circulation flow provides the similarity requirement. In this step, the similarity parameters are conserved in the test facility, while the time scale, geometric requirement, and similarity requirement of the primal thermal hydraulic parameters are determined (Nuclear Energy Agency, 2017, p. 91). Similarity parameters for single-phase and two-phase flow are listed in Table 11 and Table 12 respectively. A comparison of scaling parameters under the same fluid conditions and operational conditions between Power-to-volume scaling and Three-level scaling are shown in Table 13.

Table 11 – Important dimensionless groups for Single-phase flow (Nuclear Energy Agency, 2017, pp. 91-92)

Similarity Parameter	Symbol	Equation
Richardson number	R	$\frac{g\beta\Delta T_o l_o}{u_o^2} = \frac{\text{Buoyancy}}{\text{Inertia force}}$
Friction number	F_i	$\left[\frac{f_w l}{d} + K\right]_i = \frac{Friction}{\text{Inertia force}}$
Modified Stanton number	St_i	$\left[\frac{4hl_o}{\rho_f c_{pf} u_o d}\right]_i = \frac{Wall\ convection}{Axial\ convection}$
Time-ratio number	T_i^*	$\left[\frac{l_o\ /\ u_o}{\delta^2\ /\ a_s}\right]_i = \frac{Transport\ time}{Conduction\ time}$
Biot number	B_{ii}	$\left[\frac{h\delta}{k_s}\right]_i = \frac{Wall\ convection}{Conduction}$
Heat source number	Q_{si}	$\left[\frac{q_s'''\ l_o}{\rho_s c_{ps} u_o \Delta T_o}\right]_i = \frac{Heat\ source}{Axial\ energy\ change}$
Pump characteristic number	F_d	$\frac{g\ \Delta H_d}{u_o^2} = \frac{Pump\ head}{Inirtia}$
Axial length scale	L_i	$\frac{l_i}{l_o}$
Flow-area scale	A_i	$\frac{a_i}{a_o}$

The subscripts *i*, f, and s in Table 11 and Table 12 means the *i*-th component of the loop, fluid, and solid respectively. The Time-ratio number and Biot number equations has the conduction depth parameter which is defined as $\delta_i = a_{si} / \xi_i$ (Nuclear Energy Agency, 2017, p. 92).

Table 12 – Similarity parameters for Two-phase flow (Nuclear Energy Agency, 2017, pp. 92-93)

Similarity Parameter	Symbol	Equation
Phase-change number (Zuber number)	N_{pch}	$\left[\frac{4\, q_o'''\, \delta\, l_o}{d\, u_o\, \rho_f\, i_{fg}}\right]\left[\frac{\Delta\rho}{\rho_g}\right]$
Sub-cooling number	N_{sub}	$\left[\frac{\Delta i_{sub}}{i_{fg}}\right]\left[\frac{\Delta\rho}{\rho_g}\right]$
Froude number	N_{FR}	$\left[\frac{u_o^2}{g\, l_o \alpha_o}\right]\left[\frac{\rho_f}{\Delta\rho}\right]$
Drift-flux number (void-quality relation)	N_{di}	$\left[\frac{u_{gj}}{u_o}\right]_i$
Time-ratio number	T_i^*	$\left[\frac{l_o\, /\, u_o}{\delta^2\, /\, a_s}\right]_i$
Thermal-inertia ratio	N_{thi}	$\left[\frac{\rho_s\, c_{ps}\, \delta}{\rho_f\, c_{pf}\, d}\right]_i$
Friction number	N_{fi}	$\left[\frac{f_w\, l}{d}\right]_i\left[\frac{1+x(\Delta\rho/\rho_g)}{(1+x(\Delta\mu/\mu_g))^{0.25}}\right]\left[\frac{a_o}{a_i}\right]^2$
Orifice number	N_{oi}	$K_i\left[1+x^{3/2}\left(\frac{\Delta\rho}{\rho_g}\right)\right]\left[\frac{a_o}{a_i}\right]^2$

The second step (or level) is the scaling of mass & energy inventory, and boundary flow (Ishii, et al., 1998, p. 188). The preservation of thermal hydraulic interactions between inter-component relations is an importance prospect for proper scaling of a system consisting of several inter-connected components. Control-volume balance equations for mass and energy provides their scaled inventory for each component. At breaks and valves (safety and depressurization values), the discharge-flow phenomena should be preserved to insure the similar histories for depressurization between the prototype and the model (Nuclear Energy Agency, 2017, p. 93).

Conserving the important thermal hydraulic phenomena occurring in each system is the aim in the last step the local phenomena scaling (Ishii, et al., 1998, p. 191). In a specific component, the required local thermal hydraulic phenomena can remain unsatisfied in spite of achieving an overall similarity of the system response from the integral scaling step. Key thermal hydraulic phenomena in the system is covered through local similarity analysis in this step. In the case of a similarity requirement obtained in the third step (local phenomena scaling analysis) being different from that of the first step (integral scaling), the conservation of the physical phenomena with higher priority is achieved by replacing the requirement from the integral scaling with the result from scaling of local phenomena (Nuclear Energy Agency, 2017, p. 93).

Table 13 – Comparison of main scaling ratios of power-to-volume and Ishii three-level scaling methods (Nuclear Energy Agency, 2017, p. 88)

Parameter	Symbol	Parameter Ratio (Model/Prototype)	
		Power-to-volume scaling	Ishii three-level scaling
Height	l_R	1	l_R
Diameter	d_R	d_R	d_R
Area	a_R	${d_R}^2$	${d_R}^2$
Volume	V_R	${d_R}^2$	$l_R\ a_R$
Core ΔT	ΔT_R	1	1
Velocity	u_R	1	${l_R}^{1/2}$
Time	t_R	1	${l_R}^{1/2}$
Gravity	g_R	1	1
Power/volume	${q_R}'''$	1	${l_R}^{-1/2}$
Heat flux	${q_R}''$	1	${l_R}^{-1/2}$
Core power	q_{Ro}	${d_R}^2$	$a_R\ {l_R}^{1/2}$
Rod diameter	D_R	1	1
Number of rods	n_R	${d_R}^2$	a_R
Flow rate	$\dot{m}_R$	${d_R}^2$	$a_R\ {l_R}^{1/2}$

The three-level scaling method is distinguished by its length scale with relaxed restriction. The scaling distortion of a small-scale test facility can be minimized in three-level scaling by implementing a proper scale length which is not possible in power-to-volume scaling method. A comparison of main scaling ratios in power-to-volume and three-level scaling

methods are shown in Table 13. From Table 13 it can be seen the scales for time and flow velocity effected by the reduced length-scale ($t_R = {l_R}^{1/2}$ and $u_R = {l_R}^{1/2}$) which generates an inevitable distortion of the local thermal hydraulic phenomena. However, it is possible to overcome the resulted distortion by satisfying the similarity requirement from the local-phenomena at the third step of three-level scaling (Nuclear Energy Agency, 2017, p. 93).

3.1.3 Hierarchical two-tiered scaling

The Hierarchical two-tiered scaling (H2TS) was developed in 1998 by Prof Zuber as a method that provides a comprehensive and systematic scaling-methodology that does not compromise practicability, auditability, traceability and is technically justifiable. The method eliminates the arbitrariness in deriving the scaling requirements by creating a hierarchy among scaling factors and scaling design or requirements, providing a quantitative estimate of the importance of the scaling factor. (D'Auria & Galassi, 2010, p. 15)

The analysis method for H2TS scaling is composed of four stages: system breakdown, scale identification, top-down scaling analysis, and bottom-up scaling analysis. A flow diagram for each stage in the hierarchy is shown in Figure 10. (Nuclear Energy Agency, 2017, p. 90)

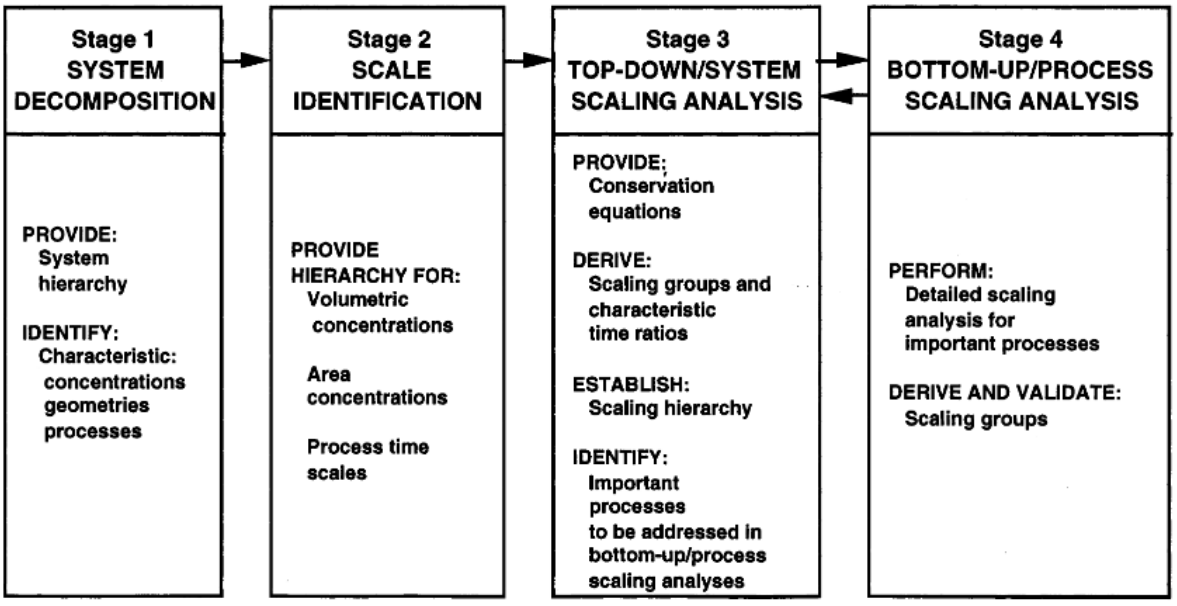

Figure 10 – Flow diagram for H2TS method stages (Zuber, et al., 1998, p. 8)

In the first stage, the system is broken down into subsystems, modules, constituents, geometrical configurations, fields, and processes. The decomposed system's architecture is

used to establish hierarchies for important transfer processes characterized by the three measurements volumetric concentration (α), spatial scale (L), and temporal scale (τ). The volumetric concentration is the volume fraction of a given constituent, the scale of the transfer area for a given process is related to the spatial scale, and the rate of transfer is governed by the temporal scale parameter. (Nuclear Energy Agency, 2017, p. 90)

In the second stage, a hierarchy is provided for the characteristic volume fraction, spatial scale, and temporal scale. The volumes of the control volume (V_{CV}), constituent (V_C), and geometrical configuration (V_{CG}) are related by the volume fractions α_C, and α_{CG} as shown in equation 1 and equation 2 respectively. (Nuclear Energy Agency, 2017, p. 90)

$$V_C = \alpha_C V_{CV} \qquad (1)$$

$$V_{CG} = \alpha_{CG} V_C \qquad (2)$$

In the case of the hierarchy for characteristic spatial scales, the characteristic length scale (L_{CG}) is defined as the ratio of the transfer area (A_{CG}) for a specific process to the volume (V_{CG}) as shown in equation 3. (Nuclear Energy Agency, 2017, p. 90)

$$\frac{A_{CG}}{V_{CG}} = \frac{1}{L_{CG}} \qquad (3)$$

Establishing the hierarchy of the temporal scale requires to define a characteristic frequency of a specific process across an area A_{CG} (ω_{CG}). It is defined as the amount of property ψ (which can be mass, momentum, or energy) contained in volume V_{CG} being changed due to a particular flux j_i across the transfer area A_{CG} as shown in equation 4. The characteristic frequency in the control volume V_{CV} (ω_i) can be related to ω_{CP} as shown in equation 5. (Nuclear Energy Agency, 2017, p. 90)

$$\omega_{CG} = \frac{j_i \, A_{CG}}{\psi \, V_{CG}} \qquad (4)$$

$$\omega_i = \frac{j_i \, A_{CG}}{\psi \, V_{CV}} = \alpha_C \, \alpha_{CG} \, \omega_{CG} \qquad (5)$$

Because the transfer processes (of mass, momentum, energy) are evaluable in terms of one parameter only, that is in terms of time, the dimensionless groups are obtained in terms of

time ratios (Zuber, et al., 1998, p. 15). By using the system response time ($\tau_{CV} = V_{CV}/Q_f$) where Q_f is the volumetric flow rate, the characteristic time ratio (Π_i) is defined as shown in equation 6 (Nuclear Energy Agency, 2017, p. 90).

$$\Pi_i = \omega_i \, \tau_{CV} = \alpha_C \, \alpha_{CG} \, \omega_{CG} \, \tau_{CG} \qquad (6)$$

In the third stage, conservation equations of mass, momentum and energy in control volume are used to establish a scaling hierarchy using top-down scaling analysis. The balance equation for a constituent "i" is shown in equation 7 in non-dimensional normalized form. (Nuclear Energy Agency, 2017, p. 90)

$$\tau_i \frac{d(V_i^* \psi_i^*)}{dt} = \Delta[Q_i^* \psi_i^*] \pm \sum_{k=1}^{m-1} (\Pi_{ik} \, j_{ik}^* \, A_{ik}^*) \qquad (7)$$

For the processes between the constituent "i" and other "$m-1$" constituent many characteristic time ratios exists as equation 7 shows and the "$\pm$" sign means the term could be either a source or a sink. As a result, evaluation in terms of time is possible for all the processes for each constituent and geometrical configuration. Additionally, ranking the processes according to their importance on the system is also possible. A scaling hierarchy based on this therefore is able to identify similarity groups between an actual model and a scaled-down facility and provides priorities for the design of the test facility, code development, and uncertainty quantification (Nuclear Energy Agency, 2017, p. 90). A list of the dominant processes for characteristic time ratios is shown in Table 14 which were used for the scaling down of the Advanced Plant Experiment (APEX) test facility (Reyes & Hochreiter, 1998, pp. 92-93).

In the fourth stage, the bottom-up scaling approach is applied. It is a detailed scaling analysis for key phenomena and processes. Important phenomena in subsystems gets identified in this stage, and the analysis sequence for the processes and the mechanisms are determined. Obtaining the scaling criteria and time constants is done by applying a step-by-step integral method for the processes. The evaluation for the relative importance of the processes is done at the end. (Nuclear Energy Agency, 2017, p. 91)

Table 14 – Characteristic time ratios for dominant processes (Reyes & Hochreiter, 1998, pp. 92-93)

Characteristic time ratio	Symbol	Equation
1ϕ natural circulation	Π_{Ri}	$\frac{\beta_T\ g\ q_c\ l_c}{\rho_{lo}\ C_{plo}\ u_{lo}^3\ a_c}$
1ϕ and 2ϕ natural circulation and LCS recirculation	Π_F	$\left(\frac{f\ l}{d_H}+K\right)_o$
2ϕ natural circulation and LCS recirculation	Π_h	$\left(\frac{h_{lg}(1-\alpha)\ \alpha\ \Delta\rho\ u_f\ a_c}{q_c}\right)_o$
2ϕ system depressurization	Π_Γ	$\left(\frac{q_{sys}}{h_{lg}\ \Sigma C_D\ G_e\ a_e}\right)_o$
CMT draining (hot wall)	$\Pi_{\Gamma,CMT}$	$\left(\frac{H_{WL}\ A_{WL}\ (T_w-T_{SAT})}{\dot{m}_{CMT}\ h_{lg}}\right)_o$
CMT draining (cold wall)	Π_{cond}	$\left(\frac{H_{LF}\ A_{Ws}\ (T_w-T_{SAT})}{\dot{m}_{CMT}\ h_{lg}}\right)_o$
CMT draining (cold wall)	Π_{HC}	$\left(\frac{H_{LF}\ \rho_1\ V_g}{\rho_s\ C_{vs}\ (R_o-R_i)\ \dot{m}_{CMT}}\right)_o$
IRWST injection	$\Pi_{m,IRWST}$	$\left(\frac{\dot{m}_{ADSI-3}+\dot{m}_{cc}}{\dot{m}_{IRWST}}\right)_o$
IRWST draining	$\Pi_{h,IRWST}$	$\left(\frac{(\dot{m}\ h)_{ADSI-3}+(\dot{m}\ h)_{cc}}{(\dot{m}\ h)_{IRWST}}\right)_o$
Downcomer fluid heatup	$\Pi_{q,DC}$	$\left(\frac{q_{DC}}{(\dot{m}\ h)_{DVI}}\right)_o$
LSC filling and recirculation	$\Pi_{m,sump}$	$\left(\frac{\dot{m}_{SL}}{\Sigma\dot{m}_{in}}\right)_o$

3.1.4 Fractional change scaling and analysis method

This method is also called Fractional Scaling Analysis (FSA). It is a systematic method that was developed as an advancement from H2TS and is based on well-established general theory. FSA ranks components and the phenomena in the components in terms of their effect on the figure of merit (FOM) or safety parameter. Additionally, it allows the synthesize of data for the same class of transients from different facilities. The multistage scaling in FSA enables the design of a scaled facility through the identification of important components and their corresponding important processes. By providing flexibility in addressing only the

important components, the facility design will be simplified in the scaling process. (Nuclear Energy Agency, 2017, p. 95)

The FSA considers two key parameters, the fractional rates of change (FRC) and fractional change metric (FCM). For a given control volume, FRC quantifies the intensity of the state variables change in response to processes (or "agents of change") that are taking place inside and at the boundaries. The fractional change of a state variable is represented for scaling by FCM parameter. In comparison with H2TS, the FRC has the role of characteristic frequency and FMC has the role of characteristic time ratio. (D'Auria & Galassi, 2010, p. 16)

3.2 Scaling distortions

Any conflict between the parameters obtained through scaling and an actual plant are referred to as scaling distortions. Ideally, a scaled-down experimental model would equally reproduce all the scaled parameters at the designated scale. In practice, the feasibility to achieve perfect scaling would be extremely limited to specific cases (D'Auria, 2017, p. 116). It is unavoidable to encounter some scaling distortions because of the hardship in matching the scaling criteria, and the shortage of understanding the scaled phenomenon (Ishii, et al., 1998, p. 209). Typically, the nature of tests is intricate and includes phenomena requiring a wide range of scaling criteria to design a scaled-down test facility (D'Auria, 2017, p. 116).

Defining similarity conditions is possible through generating a list of nondimensional groups which are obtained using nondimensional equations and laws. Unfortunately, in the design of a scaled-down facility it is not possible to match all of the similarity conditions. Once the decision to preserve the most relevant processes is made distortions will start to appear. One of the most crucial objectives of current scaling development is analysis and justification of such generated distortions (D'Auria, 2017, pp. 116-117). For a specific transfer-process, the characteristic time ratio can be utilized to determine scaling distortion between a prototype and a test facility (model) as shown in equation 8 (Nuclear Energy Agency, 2017, p. 91).

$$D = \frac{[\Pi_i]_{prototype} - [\Pi_i]_{model}}{[\Pi_i]_{prototype}} \qquad (8)$$

3.3 Using system codes in scaling analysis

Complex transient analysis involved in scaling could benefit from using system codes. For instance, the man-power cost in H2TS and FSA which is done by hand could be partially salvaged with the aid of system codes. Regardless though, scaling analysis should not be substituted with system codes because they are tools to be used to assist the scaling analysis and solving problems. To illustrate this point, consider a phase of a transient in a scaling process. Preliminary simulations using system codes could make it easier to identify the transient's phase without the need of simulation in a test facility. (D'Auria, 2017, p. 117)

Additionally, main processes could be identified using system codes. Furthermore, the change that may occur for the relatively important processes after transition could be predicted with system codes. Moreover, system codes could investigate phenomena of less importance that might occur. Attention might be required for such cases nonetheless. (D'Auria, 2017, p. 117)

4 SCALING DOWN THE STEAM GENERATOR DESIGNS

In this section, the H2TS method is applied on the vertical, horizontal, and helical SGs. Firstly, preliminary calculations were done using a 1% reactor core thermal power for the vertical and horizontal SGs, and normal operation situation in the helical SG. Then the hierarchy is established for all the SGs followed by the scaling equations analysis and the distortion calculation. The characteristic time ratios of concern are chosen from Table 14 which were derived for the APEX facility (Reyes & Hochreiter, 1998, pp. 92-93).

4.1 Preliminary calculations

After 3 hours of reactor shutdown, the reference reactor conditions with the EPR (vertical SG) and AES-2006 (horizontal SG) could be assumed to operate at 1% of their nominal thermal power due to decay heating. During the shutdown, the flow in the primary side is a single-phase natural circulation and the pressure remains nominal. Consequently, cold leg temperature drops to secondary side saturation temperature, and the mass flow rate is low with natural circulations. The mass flow rate in this case is calculated using the quantity of heat from the reactor (the 1% of nominal operation power) for both SGs. On the other hand, the helical SG of NuScale reactor during an accident situation is not assumed to be involved. The mass flow rate in that case is calculated based on normal operation situation with the model considering counter current flow heat exchange. Summary of characteristics of considered power plants is shown in Table 15.

Table 15 – Summary table for characteristics of considered power plants

	Unit	**EPR**	**AES-2006**	**NuScale**
Nominal thermal power	MW	4300	3200	160
1% power	MW	43	32	-
Number of loops	loop	4	4	2
Primary side pressure	Bars	155	162	127.5
Secondary side pressure	Bars	78	68	34.5
Secondary side pressure at 1% power	Bars	90	78 estimated	-
Cold leg nominal temperature (primary)	℃	296	298.2	258.3
Hot leg nominal temperature (primary)	℃	329	328.9	283.8
Saturation temperature (primary side)	℃	344.8	348.3	329.3
Reactor coolant pump volume flow rate	m^3/s	7.8694	5.97	-
Number of tubes in SG	tubes	5980	10978	1380
Feedwater temperature	℃	230	227	204
Feedwater mass flow rate	kg/s	2443	1780	67.04

Before using the data in Table 15 for the scaling, each SG requires some preliminary calculations. Considerations for the SG models also needs to be taken into account. The following sub-sections cover these calculations and considerations.

4.1.1 Vertical SG of EPR calculations

The MOTEL is designed to have the same thermal power core for the modular SG designs, therefore the core power for all SGs will be the same. The heating power value is fixed at the available power in LUT which is 1 MW. Table 16 includes the primary and secondary side's pressures. The hot leg temperature in the primary side is assumed to be subcooled by 10 degrees below the saturation temperature at the primary side's pressure. The live steam temperature in the secondary side would be the saturation temperature at the secondary side's pressure (because water should be boiling on the secondary side even during shutdown conditions). The cold leg temperature is assumed to reach the live steam's temperature.

Table 16 – Modular SG design assumptions

Parameter	Unit	Value
Thermal power of the core	MW	1
Primary side pressure	Bars	40
Secondary side Pressure	Bars	25
Hot leg temperature at the primary side	℃	240
Live steam temperature at the secondary side	℃	224

The first step is the determination of the 1-phase natural circulation mass flow rate on the primary side of the EPR according to equation 9 below.

$$\dot{m} = \left(\frac{\rho_{avg}\ \beta_T\ q_c\ g\ H}{C_p\ F}\right)^{\frac{1}{n+1}} = \left(\frac{\rho_{avg}\ \beta_T\ q_c\ g\ H}{C_p\ F}\right)^{\frac{1}{3}},\ if\ n = 2 \qquad (9)$$

Where ρ_{avg} is the average density, β_T is the thermal expansion coefficient of the fluid in the SG's tubes, q_c is the thermal power generated in the core, g is gravity constant ($9.81\ m/s^2$), H is the height difference between the center point of the core and the SG (approximately 15 meters in EPR), C_p is the isobaric specific heat, and F is the total loss coefficient.

Equation 9 cannot be applied directly because of the missing F factor, which is the total loss coefficient. It could be estimated from the nominal EPR reactor operation using the

mass flow rate and the primary coolant pump pressure difference according to equation 13 (the calculation can be found in the appendix). The same estimated value then is applied in equation 9 and the results are listed in Table 17.

$$(\Delta P)_{friction} = (\Delta P)_{pump} \quad (10)$$

$$(\Delta P)_{friction} = F\,\dot{m}^2 \quad (11)$$

$$(\Delta P)_{pump} = \rho_{avg}\, g\, H_{pump} \quad (12)$$

$$\Longrightarrow F = \frac{\rho_{avg}\, g\, H_{pump}}{\dot{m}^2} \quad (13)$$

Where $(\Delta P)_{friction}$ is the pressure loss because of friction, $(\Delta P)_{pump}$ is the pressure loss because of pumps, and H_{pump} is the pump head which is 100.2 meters (TVO, 2010, p. 26).

Table 17 – 1-phase steady state natural circulation mass flow rate calculation for the primary side of the EPR running at 1% power at average temperature 312.5 ℃ and 155 bars pressure

Parameter	**Symbol**	**Unit**	**Value**
Average density	ρ_{avg}	kg/m^3	694.622
Thermal expansion coefficient	β_T	$1/K$	0.003598
Thermal power of the core	q_c	J/s	43 $(10)^6$
Gravity constant	g	m/s^2	9.81
Elevation between middle of core and SG	H	m	15
Specific heat	C_p	$J/(kg.K)$	5868.7
Total loss coefficient	F	$1/kg.m$	0.0015358
Calculated mass flow rate (total)	$(\dot{m})_{total}$	kg/s	1206.11
Mass flow rate per SG	$(\dot{m})_{per\ SG}$	kg/s	301.517

The calculated mass flow rate in Table 17 is the total mass flow rate required for 1-phase natural circulation in the primary side of the EPR. Finding the natural circulation velocity in the primary side is calculated according to equation 14 where u_{lo} is the calculated velocity, n_{tubes} is the total number of tubes in one SG, and n_{loops} is the number of loops in the reactor. The calculation data and results are shown in Table 18.

$$\dot{m} = \frac{\pi}{4}(d_{tube})^2\, u_{lo}\, \rho_{avg}\, n_{tubes}\, n_{loops} \quad (14)$$

Table 18 - Natural circulation velocity calculation in EPR

Parameter	Symbol	Unit	Value
Mass flow rate (total)	$\dot{m}$	kg/s	1206.11
Tube diameter (inner diameter)	d_{tube}	m	0.01687
Average fluid density (primary side)	ρ_{avg}	kg/m^3	694.622
Number of tubes	n_{tubes}	$tube$	5980
Number of loops	n_{loops}	$loop$	4
Velocity of flow	u_{lo}	m/s	0.3248

The next step is to determine the height of the SG model and the flow velocity in it. The chosen SG height scale is 1:4 and then the velocity could be scaled down as ${l_R}^{1/2}$ according to Ishii's method as previously shown in Table 13. The results of the height and velocity scaling are listed in Table 19.

Table 19 - Height and velocity scaling ratios for vertical SG model

Parameter	Scaling ratio	Value	
		Prototype	Model
Height (l_R)	1: 4	15 m	3.75 m
Velocity (primary side)	1: 2	0.3248	0.1624 m/s

After finding the velocity of the flow in the SG model, the next parameter to find is the mass flow rate using energy balance equation on the primary side according to equation 15 and data from Table 16. The calculation parameters and result are listed in Table 20.

$$q_c = \dot{m}\, C_p (T_{hot} - T_{cold}) \qquad (15)$$

Table 20 – Vertical SG model primary side's mass flow rate calculations (at 40 bars)

Parameter	Symbol	Unit	Value
Thermal power of the core	q_c	J/s	$(10)^6$
Specific heat	C_p	$J/(kg.K)$	4688.1
Hot leg temperature	T_{hot}	℃	240
Cold leg temperature (equals live steam temp)	T_{cold}	℃	224
Mass flow rate in primary side (total)	$\dot{m}$	kg/s	13.33

The secondary side's mass flow rate can be easily determined after obtaining all the necessary information from the primary side. By applying an energy balance in the SG (as a heat exchanger) with a temperature raise in the secondary side for the feedwater form 40 ℃ to reach the saturation temperature and assuming no losses, the mass flow rate in the secondary side is calculated according to equation 16 and the results are listed in Table 21.

$$\left[\dot{m}\, C_p\, (T_{hot} - T_{cold})\right]_{primary} = \left[\dot{m}\, (h_{steam} - h_{feedwater})\right]_{secondary} \qquad (16)$$

Table 21 – Vertical SG model secondary side's cold leg calculation parameters and results (at 25 bars)

Parameter	Symbol	Unit	Value
Feedwater temperature	$T_{feedwater}$	℃	70
Feedwater enthalpy	$h_{feedwater}$	kJ/kg	295.04
Live steam temperature	T_{steam}	℃	224
Live steam enthalpy	h_{steam}	kJ/kg	2802.0
Mass flow rate in secondary side (total)	$(\dot{m})_{sec}$	kg/s	0.399

The last step is to determine the number of tubes in the SG model. The diameter of the tubes in the SG model will be assumed to be conserved same as the original EPR dimension (outer diameter is 19.05 mm and 1.09 mm thickness). The triangular pitch between the tubes is also going to be conserved (27.43 mm). Equation 14 then is applied to determine the required amount of tubes and the results are shown in Table 22.

Table 22 – Number of tubes calculation parameters for vertical SG model

Parameter	Symbol	Unit	Value
Mass flow rate (total)	$(\dot{m})_{total}$	kg/s	13.33
Tube diameter (inner diameter)	d_{tube}	m	0.01687
Velocity of flow	u_{lo}	m/s	0.1624
Fluid density (primary side)	ρ	kg/m^3	825.5
Number of loops	n_{loops}	$loop$	2
Number of tubes per SG	n_{tubes}	$tube$	222

The calculated 222 tubes in each SG are distributed as shown in Figure 11. The shortest and longest SG tubes and their corresponding dimensions are shown in Figure 12.

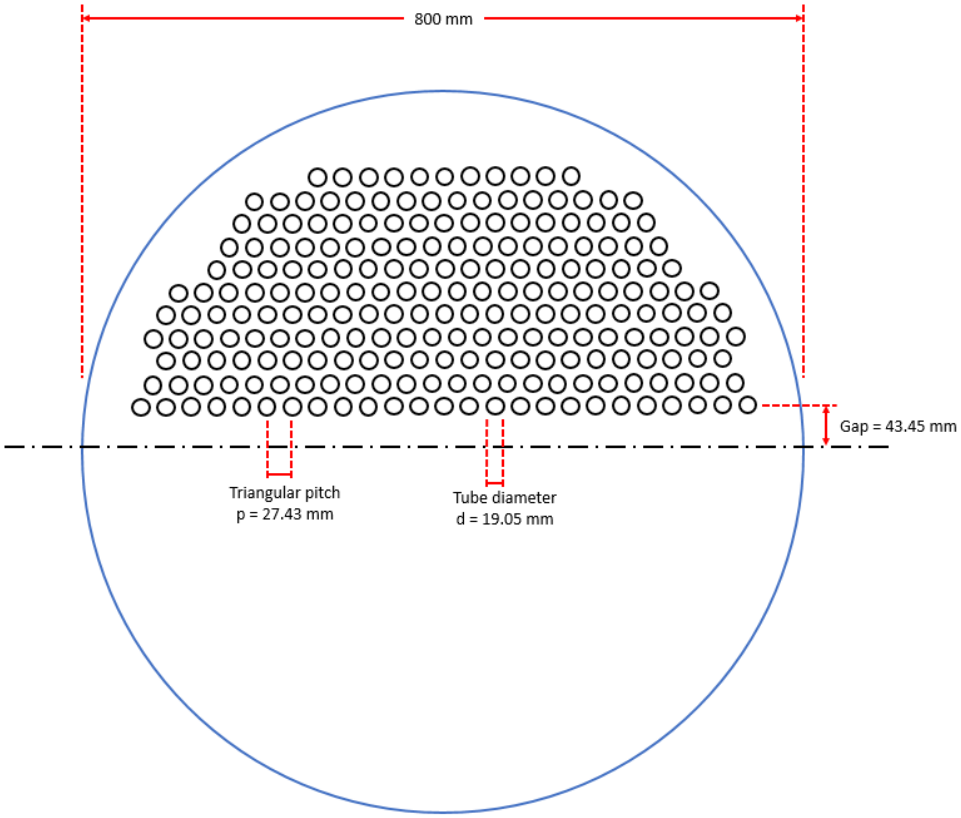

Figure 11 – Proposed tubes distribution for the vertical SG model (totally there are 222 tubes)

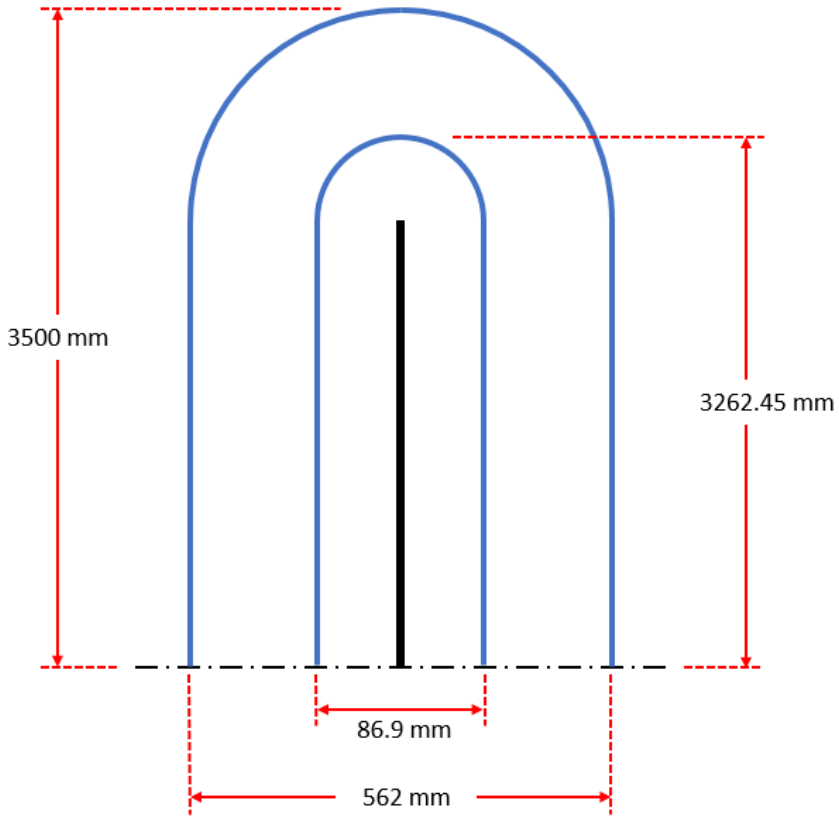

Figure 12 – Proposed dimensions for shortest and longest tubes (shown in blue) for the vertical SG model

4.1.2 Horizontal SG of AES-2006 calculations

The same initial assumptions from Table 16 are applied for the horizontal SG model and equation 9 is used to estimate the 1-phase natural circulation mass flow rate and the result is shown in Table 23. Equation 13 is used to determine the total loss coefficient (in the appendix) with an approximate 10 meters height difference between the center point of the core and the SG and 62.2 meters pump head (IAEA, 2011, p. 30).

Table 23 - 1-phase steady state natural circulation mass flow rate calculation for the primary side of the AES-2006 running at 1% power at average temperature 313.55 ℃ and 162 bars pressure

Parameter	Symbol	Unit	Value
Average density	ρ_{avg}	kg/m^3	694.465
Thermal expansion coefficient	β_T	$1/K$	0.003472
Thermal power of the core	q_c	J/s	32 $(10)^6$
Gravity constant	g	m/s^2	9.81
Elevation between middle of core and SG	H	m	10
Specific heat	C_p	$J/(kg.K)$	5829.7
Total loss coefficient	F	$1/kg.m$	0.001324
Calculated mass flow rate (total)	$(\dot{m})_{total}$	kg/s	993.5
Mass flow rate per SG	$(\dot{m})_{per\ SG}$	kg/s	248.375

The calculated mass flow rate in Table 23 is the total mass flow rate required for 1-phase natural circulation in the primary side of the AES-2006. Finding the natural circulation velocity in the primary side is calculated according to equation 14 and results are shown in Table 24.

Table 24 – Natural circulation velocity calculation for AES-2006

Parameter	Symbol	Unit	Value
Mass flow rate (total)	$\dot{m}$	kg/s	993.5
Tube diameter (inner diameter)	d_{tube}	m	0.013
Average fluid density (primary side)	ρ_{avg}	kg/m^3	694.465
Number of tubes	n_{tubes}	$tube$	10978
Number of loops	n_{loops}	$loop$	4
Velocity of flow	u_{lo}	m/s	0.24545

The next step is to scale-down the SG dimensions and velocity in the AES-2006. The SG's shell length will be reduced with a 1:4 scaling ratio and the average tube length will be assumed to be the same size as the shell's length. The height of the horizontal SG would be the SG's shell diameter and will have 1:2 scaling ratio in the SG model and the velocity in the SG model is scaled down as ${l_R}^{1/2}$ according to Ishii's method as previously shown in Table 13. The results of the dimensions and velocity scaling are listed in Table 25.

Table 25 - Dimensions and velocity scaling ratios for Horizontal SG model

Parameter	**Scaling ratio**	**Value**	
		Prototype	**Model**
Height (l_R) = Shell diameter (inner)	1: 2	4.2 m	2.1 m
SG shell length (inner)	1: 4	13.82 m	3.455 m
Approximated tube length	1: 4	13.82 m	3.455 m
Velocity (primary side)	1: $\sqrt{2}$	0.24545	0.17356

After finding the velocity of the flow in the SG model, the next parameter to find is the mass flow rate using energy balance equation on the primary side according to equation 15 and data from Table 16. The calculation parameters and result are listed in Table 26.

Table 26 – Horizontal SG model primary side's mass flow rate calculations (at 40 bars)

Parameter	**Symbol**	**Unit**	**Value**
Thermal power of the core	q_c	J/s	$(10)^6$
Specific heat	C_p	$J/(kg.K)$	4688.1
Hot leg temperature	T_{hot}	℃	240
Cold leg temperature (equals live steam temp)	T_{cold}	℃	224
Mass flow rate in primary side (total)	$\dot{m}$	kg/s	13.33

The next step is to determine the number of tubes in the SG model. The diameter of the tubes in the SG model will be assumed to be conserved same as the original AES-2006 dimension (outer diameter is 16.00 mm and 1.50 mm thickness). Equation 14 then is applied to determine the required amount of tubes and the results are shown in Table 27.

Table 27 – Number of tubes calculation parameters for horizontal SG model

Parameter	Symbol	Unit	Value
Mass flow rate (total)	$(\dot{m})_{total}$	kg/s	13.33
Tube diameter (inner diameter)	d_{tube}	m	0.013
Velocity of flow	u_{lo}	m/s	0.17356
Fluid density (primary side)	ρ	kg/m^3	825.5
Number of loops	n_{loops}	$loop$	2
Number of tubes per SG	n_{tubes}	$tube$	350

The approach to find the distribution of the tubes inside the AES-2006 can be found in the appendix. The same approach is used to estimate the tubes distribution and dimensions inside the SG model. The model has 2 sets of tubes, one contains 70 tubes (outer side) and the other contains 105 tubes (inner side) from 1 side. Because the hot and cold collectors have 2 sides, the number of tubes then becomes 350 which covers both the front and back of the collectors. The dimensions inside the horizontal SG model are shown in Figure 15 with $22mm \times 72mm$ rectangular pitch.

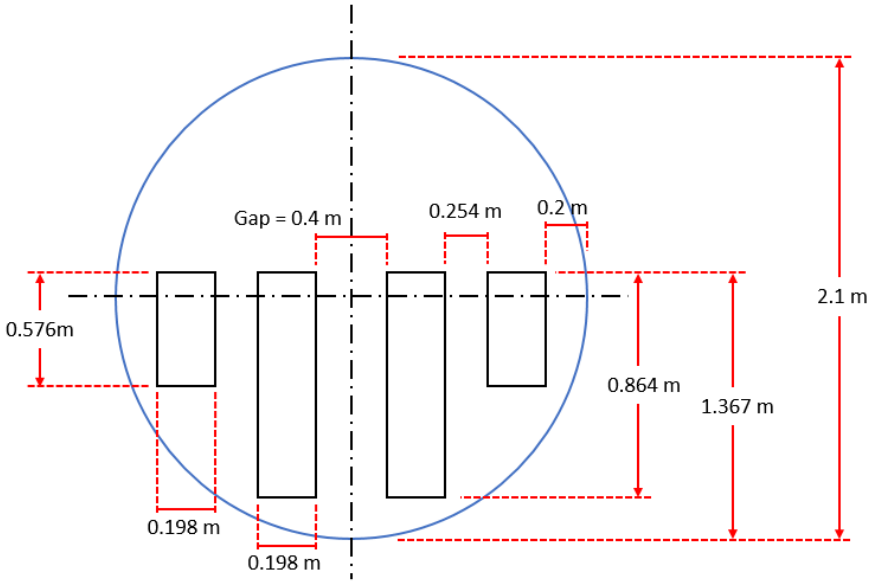

Figure 13 - Proposed dimensions for the horizontal SG model (figure is not to scale)

There is one more parameter to be conserved for the horizontal SG model which is described in equation 17. The factor of characteristic pressure differences F_{HSG} is the hydrostatic pressure difference in the SG collectors versus average pressure loss along heat exchanger tubes. By conserving the F_{HSG} value between the AES-2006 SG and the SG model, the height

of tube bundle's bank H_{TB} can be estimated for the SG model. An illustration of the tube bank is shown in Figure 13.

$$F_{HSG} = \frac{\Delta\rho \; g \; H_{TB}}{\left(f \; \frac{L_t}{d_{tube}} + K\right)\left(\frac{1}{2} \; \rho_{avg} \; (u_{lo})^2\right)} \qquad (17)$$

Where H_{TB} is the tube bundle height, f is the friction factor, L_t is the average tube length from the hot collector to the cold collector, d_{tube} is the tube's inner diameter, and K is the sum of form losses.

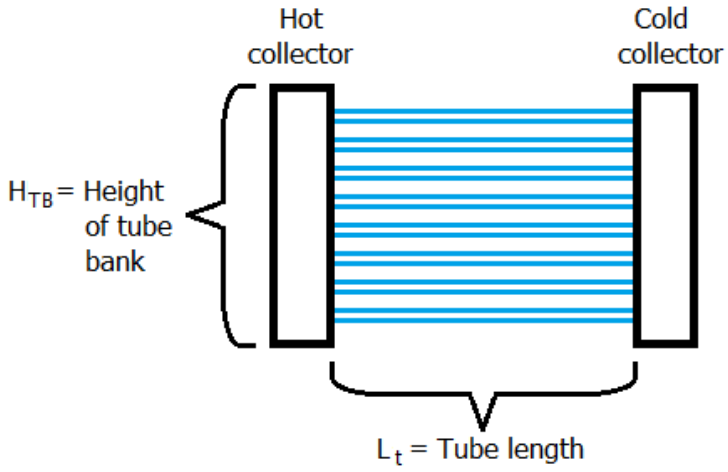

Figure 14 – Illustration of the horizontal SG's tube bank for the hot and cold collectors

The friction factor f is estimated using rough pipe (tube's relative roughness = 0.02) assumption and Moody diagram (Incropera, et al., 2006, p. 491). Reynolds number Re is calculated using equation 18 where μ is the dynamic viscosity. The parameters and results from equations 17 and 18 for the SG scaled-down model are shown in Table 28.

$$Re = \frac{\rho_{avg} \; u_{lo} \; d_{tube}}{\mu} \qquad (18)$$

The value of the sum of form losses K from Table 28 was estimated using Figure 14 and the assumptions below:

- Pipe entrance: Slightly rounded (value = 0.2)
- Pipe exit: Slightly rounded (value = 1.0)

- Elbows: Totally there are 6 elbows, 3 on each side. Each elbow is assumed to be rounded at 45 degrees (each has a value = 0.4)
- Sum of form losses $K = 0.2 + 1.0 + [(0.4)(6)] = 3.6$

Table 28 – Factor of characteristic pressure differences calculation parameters and results for horizontal SG

Parameter	Symbol	Unit	Value	
			AES-2006	Model
Cold leg density	ρ_{cold}	kg/m^3	731.48	836.43
Hot leg density	ρ_{hot}	kg/m^3	657.45	814.06
Density difference	$\Delta\rho$	kg/m^3	74.03	22.37
Gravity constant	g	m/s^2	9.81	9.81
Tube bank height	H_{TB}	m	2.3	1.367
Tube length	L_t	m	13.82	3.455
Tube diameter (inner)	d_{tube}	m	0.013	0.013
Sum of form losses	K	$-$	3.6	3.6
Average density	ρ_{avg}	kg/m^3	694.465	825.245
Flow velocity	u_{lo}	m/s	0.24545	0.17356
Cubic velocity	$(u_{lo})^2$	$(m/s)^2$	0.06024	0.03012
Dynamic viscosity	μ	$Pa.s$	0.0000834	0.000115
Reynold number	Re	$-$	$2.66(10)^4$	$1.62(10)^4$
Friction factor	f	$-$	0.05	0.051
Char. pressure difference	F_{HSG}	s^2	1.4069	

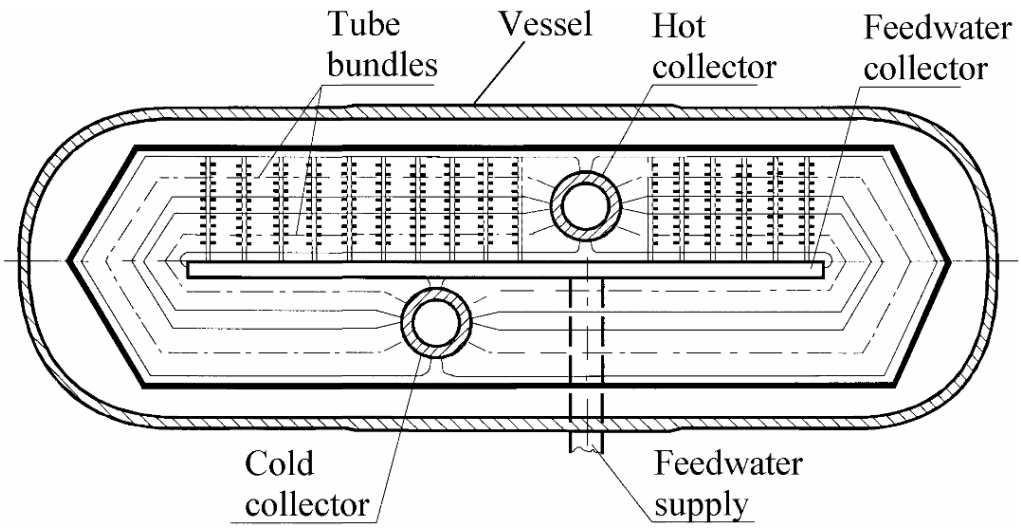

Figure 15 – Cross-sectional top view of PGV-1000MKP horizontal SG (Dolganov & Shishov, 2012, p. 4)

4.1.3 Helical SG of NuScale calculations

As mentioned earlier, during an accident situation, the helical SG in the NuScale is not assumed to be involved. Therefore, the calculation is done in normal operation situation considering counter current flow heat exchange (once through SG). The SG design requirements are shown in Table 29.

Table 29 – Helical SG design assumptions

Parameter	Unit	Value
Thermal power of the core	MW	1
Primary side pressure	Bars	40
Secondary side Pressure	Bars	15
Hot leg temperature (primary side)	℃	230
Cold leg temperature (primary side)	℃	204.5
Feedwater temperature (secondary side)	℃	70
Live steam temperature (secondary side)	℃	228.3
Superheating temperature (secondary side)	℃	30

The hot leg temperature in the primary side is assumed to be 20 degrees below the saturation temperature at the primary side's pressure, and the cold leg temperature is assumed to be 25.5 degrees below the hot leg temperature. On the secondary side, the live steam is assumed to be superheated to 30 degrees above the saturation temperature of the secondary side. The mass flow rate in the primary side is found using equation 15 and the mass flow rate in the secondary side is found using energy balance according to equation 16. The results from the calculation are listed in Table 30.

Table 30 – Mass flow rate for the helical SG model

Parameter	Symbol	Unit	Value
Thermal power of the core	q_c	J/s	$(10)^6$
Calculated mass flow rate (primary side)	$(\dot{m})_{prim}$	kg/s	8.56
Specific heat (primary side)	$(C_p)_{prim}$	$J/(kg.K)$	4580
Temperature difference in the primary side	$(\Delta T)_{prim}$	℃	25.5
Calculated mass flow rate (secondary side)	$(\dot{m})_{sec}$	kg/s	0.388
Live steam enthalpy (secondary side)	h_{steam}	kJ/kg	2871.2
Feedwater enthalpy (secondary side)	$h_{feedwater}$	kJ/kg	294.22

4.2 Establishing the hierarchy

Establishing a hierarchal architecture for the SGs is achieved by physically decomposing the SGs into their sub-parts as illustrated in Figure 16. The decomposition scheme is applied for all the 3 different SGs because they all share the same internal parts in different configurations.

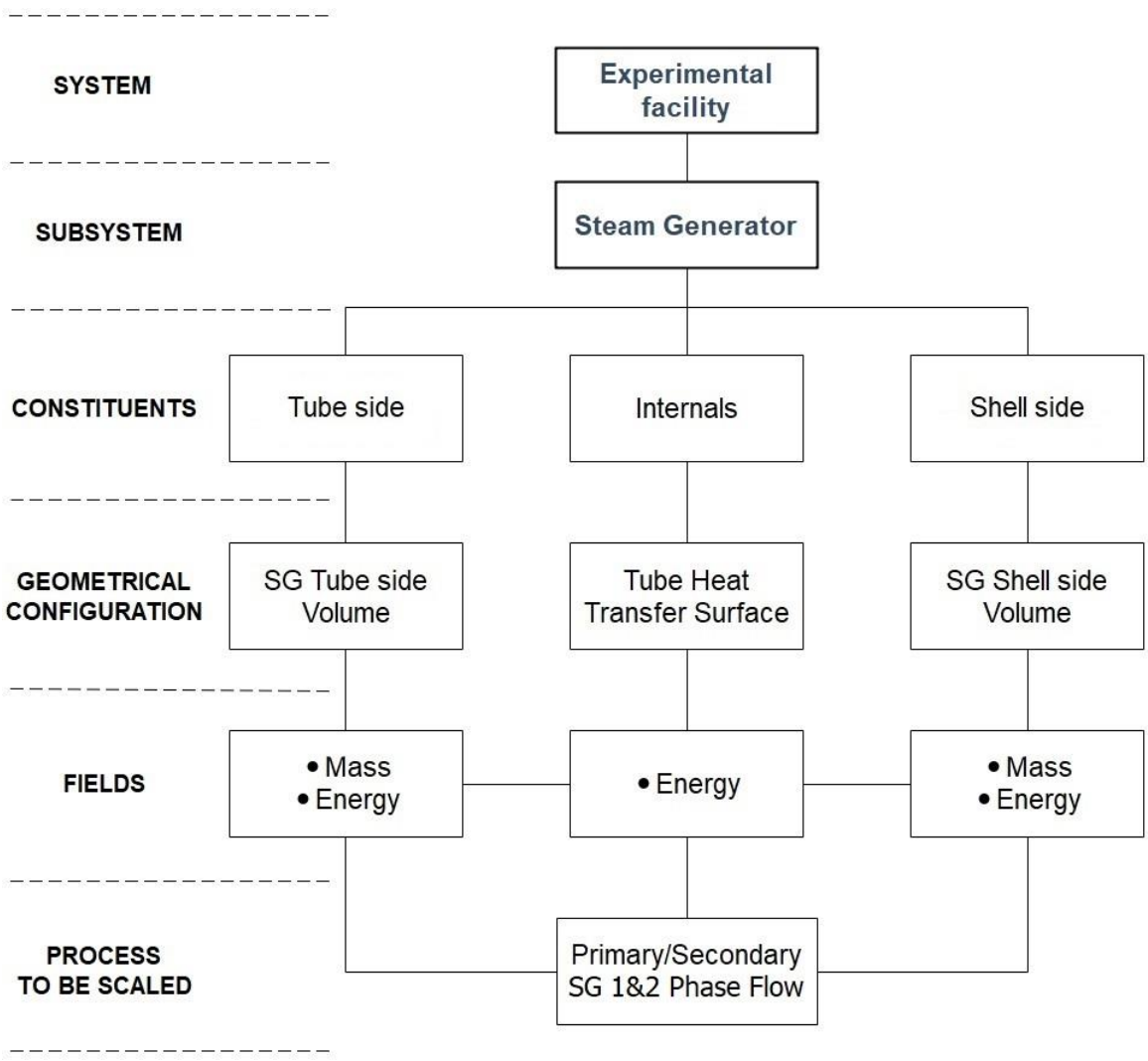

Figure 16 – SG decomposition and hierarchy

The decomposition shown in Figure 16 starts from the system which is the experimental facility. The system then can be divided into many interacting subsystems. Since only the SG is the part of concern in this work, all other subsystems in the hierarchy were ignored. The SG is then divided into its interacting constituents (materials): the tubes, shell, and internals. Each constituent is further characterized by a geometrical configuration. Field equations (conservation equations of mass, energy, and momentum) describes each

geometrical configuration. Finally, each field can be characterized by processes that needs to be scaled.

The chosen processes to be scaled where based on natural circulation of flow in the primary side of the SG. The next step would be the scaling analysis based on the suitable characteristic time ratios for the SG which were previously addressed in Table 14.

4.3 Scaling equations analysis

Ideally, similarities between processes occurring at full-scale and scaled-down test facility would be fully maintained in a scaling process. In reality, complete processes preservation is not achievable. Therefore, the approach is to optimize the similitude for greatest processes of interest. In this work, natural circulation was chosen as the phenomena to be preserved and therefore the characteristic time ratios for 1-phase and 2-phase natural circulations will be optimized for the vertical, horizontal, and helical SGs.

4.3.1 1-phase natural circulation

The characteristic time ratio for 1-phase natural circulation is shown in equation 19 below:

$$\Pi_{Ri} = \frac{\beta_T \; g \; q_c \; l_c}{\rho_{lo} \; C_{plo} \; u_{lo}^3 \; a_c} \qquad (19)$$

Where β_T is the thermal expansion coefficient of the fluid in the SG's tubes, g the gravitational acceleration, q_c the quantity of heat (the heat generated from the core, or the thermal power), l_c the axial length for the tubes, ρ_{lo} the liquid density in the primary side, C_{plo} the specific heat of the primary side's liquid, u_{lo} the velocity of the flow in the primary side, and a_c the cross-section flow area.

To achieve the similarity, equation 19 needs to be calculated twice for each SG type, one time for the full-scale prototype and the second time for the scaled-down SG. There are 3 types of SGs (vertical, horizontal, and helical), therefore the equation is solved 6 times in total. The parameters in the equation were chosen according to the points below:

- The thermal expansion coefficient β_T of the fluid in the SG's tubes will be based on the operating pressure and average temperature in the primary side of the SGs.
- Gravitational acceleration g is constant and equals 9.81 m/s.
- The quantity of heat q_c is the 1% of the core's thermal power after shutdown in the vertical and horizontal SGs. In the helical SG, it is calculated using the mass flow rate according to equation 15.
- The axial length l_c for the vertical SG is assumed to be the average tube length from the inlet point to the outlet point. The horizontal SG tube length would be the horizontal length for the tube from the hot collector to the cold collector. In the helical SG, this length is considered as the height the helical coil covers.
- The density ρ_{lo} is the fluid density in the primary side at an average temperature of the hot leg and the cold leg.
- The specific heat C_{plo} of the primary side's liquid at an average temperature of the hot leg and the cold leg.
- The fluid velocity u_{lo} in the vertical and horizontal SGs it is the scaled-down velocity in Table 19 and Table 25 respectively. In the helical SG, velocity is calculated from the mass flow rate equation in the primary side according to equation 14.
- The cross-section flow area a_c is the total flow area in the SG of the primary side. It is the total flow area in all the tubes of the SG.

4.3.2 2-phase natural circulation

The characteristic time ratio for 2-phase natural circulation is shown in equation 20 below:

$$\Pi_h = \left(\frac{h_{lg}(1-\alpha)\ \alpha\ \Delta\rho\ u_f\ a_c}{q_c} \right)_o \qquad (20)$$

Where h_{lg} is the latent heat of vaporization, α the vapor volume fraction, $\Delta\rho$ the density difference between the liquid phase and gas phase at the same temperature and pressure, u_f the fluid velocity in the primary side, a_c the cross-section flow area, and q_c the quantity of heat (the heat generated from the core, or the thermal power).

As previously shown for 1-phase natural circulation, equation 20 for 2-phase natural circulation needs to be calculated 6 times totally, 3 times for the full-scale SGs and 3 times

for the scaled-down SGs. The parameters in the equation were chosen according to the following points:

- The latent heat of vaporization h_{lg} is based on the primary side's operating pressure.
- The vapor volume fraction α is the % of the gas phase in the fluid, where 0% means the fluid is completely liquid and 100% is completely gaseous. In the similarity calculations, the vapor volume fraction between the prototype and the scaled-down model must be set as equal.
- The density difference $\Delta\rho$ is the difference between the densities of liquid phase and gas phase of the primary side at the same average temperature (between the hot leg and the cold leg) and operating pressure.
- The fluid velocity u_f is equal to the flow velocity u_{lo} in the primary side. In the vertical and horizontal SGs it is the scaled-down velocity in Table 19 and Table 25 respectively. In the helical SG, velocity is calculated from the mass flow rate equation in the primary side according to equation 14.
- The cross-section flow area a_c is similar to the value from the 1-phase natural circulation.
- The quantity of heat q_c is similar to the value from the 1-phase natural circulation.

4.4 Characteristic time ratios calculations

After acquiring the natural circulation equations, the next step is to find out the values for each SG. The calculation is firstly done for the full-scale prototype at 1% operating power then the values for the mass flow rate, the number of tubes, and the tube's diameter from the preliminary calculations (section 4.1) were used for scaled-down model. The data and results are listed based on the characteristic time ratio and the SG type. Table 31 and Table 32 shows the calculation parameters for the characteristic time ratios of 1-phase and 2-phase natural circulation for the vertical SG designs, Table 33 and Table 34 shows the same parameters for the horizontal SG designs, and Table 35 and Table 36 shows the same parameters for the helical SG designs.

Table 31 – 1-phase natural circulation characteristic time ratio parameters for vertical SGs calculated at an average temperature of 316.175 ºC and a pressure of 155 bars for the prototype, and an average temperature of 232 ºC and a pressure of 40 bars for the model

Parameter	Unit	Vertical SG	
		Full scale prototype	Scaled-down model
β_T	$1/K$	0.00361	0.00169
g	m/s^2	9.81	9.81
q_c	J/s	4.3 $(10)^6$	$(10)^6$
l_c	m	30	7.5
ρ_{lo}	kg/m^3	689.99	836.77
C_{plo}	$J/(kg.K)$	5973	4584.4
u_{lo}	m/s	0.3248	0.1624
a_c	m^2	1.337	0.04962
$\dot{m}$	kg/s	1198.23	13.48
ΔT_o	K	25.65	16
n_{tubes}	$-$	5980	222
p_{tri}	mm	27.43	27.43
d_{tube}	mm	19.05	19.05
S_{tube}	mm	1.09	1.09
a_{tube}	m^2	2.235 $(10)^{-4}$	2.235 $(10)^{-4}$
Π_{Ri}	$-$	242.026	152.510
D	$-$	0.36986	

Table 32 – 2-phase natural circulation characteristic time ratio parameters for vertical SGs calculated at an average temperature of 316.175 ºC and a pressure of 155 bars for the prototype, and an average temperature of 232 ºC and a pressure of 40 bars for the model

Parameter	Unit	Vertical SG	
		Full scale prototype	Scaled-down model
h_{lg}	J/kg	965.8 $(10)^3$	1713.5 $(10)^3$
α	$-$	5%	5%
$\Delta\rho$	kg/m^3	588.07	816.68
u_f	m/s	0.3248	0.1624
a_c	m^2	1.337	0.04962
q_c	J/s	4.3 $(10)^6$	$(10)^6$
Π_h	$-$	0.2724	0.5357
D	$-$	-0.96657	

Table 33 – 1-phase natural circulation characteristic time ratio parameters for horizontal SGs calculated at an average temperature of 311.075 °C and a pressure of 162 bars for the prototype, and an average temperature of 232 °C and a pressure of 40 bars for the model

Parameter	Unit	Horizontal SG	
		Full scale prototype	Scaled-down model
β_T	$1/K$	0.00326	0.00169
g	m/s^2	9.81	9.81
q_c	J/s	$32\ (10)^6$	$(10)^6$
l_c	m	13.82	3.455
ρ_{lo}	kg/m^3	703.89	836.77
C_{plo}	$J/(kg.K)$	5744.3	4584.4
u_{lo}	m/s	0.24545	0.17356
a_c	m^2	1.457	0.0465
$\dot{m}$	kg/s	1006.996	13.494
ΔT_o	K	35.65	16
n_{tubes}	$-$	10978	108
p_{rect}	mm	22×24	22×72
d_{tube}	mm	16.00	16.00
S_{tube}	mm	1.50	1.50
a_{tube}	m^2	$1.327\ (10)^{-4}$	$1.327\ (10)^{-4}$
Π_{Ri}	$-$	162.336	61.478
D	$-$	0.62129	

Table 34 – 2-phase natural circulation characteristic time ratio parameters for horizontal SGs calculated at an average temperature of 311.075 °C and a pressure of 162 bars for the prototype, and an average temperature of 232 °C and a pressure of 40 bars for the model

Parameter	Unit	Horizontal SG	
		Full scale prototype	Scaled-down model
h_{lg}	J/kg	$916.36\ (10)^3$	$1713.5\ (10)^3$
α	$-$	5%	5%
$\Delta\rho$	kg/m^3	594.16	816.68
u_f	m/s	0.24545	0.17356
a_c	m^2	1.457	0.0465
q_c	J/s	$32\ (10)^6$	$(10)^6$
Π_h	$-$	0.289	0.536
D	$-$	-0.85416	

Table 35 – 1-phase natural circulation characteristic time ratio parameters for helical SGs calculated at an average temperature of 271.05 ºC and a pressure of 127.5 bars for the prototype, and an average temperature of 217.25 ºC and a pressure of 40 bars for the model

Parameter	Unit	Helical SG	
		Full scale prototype	Scaled-down model
β_T	$1/K$	0.00216	0.00152
g	m/s^2	9.81	9.81
q_c	J/s	160 $(10)^6$	$(10)^6$
l_c	m	2.591	1.296
ρ_{lo}	kg/m^3	776	845
C_{plo}	$J/(kg.K)$	5000	4580
u_{lo}	m/s	5.0269	0.2064
a_c	m^2	1.622	0.0491
$\dot{m}$	kg/s	1254.902	8.56
ΔT_o	K	25.5	25.5
$d_{channel}$	m	1.50	0.25
d_{rod}	m	0.215	0
a_{tube}	m^2	1.622	0.0491
Π_{Ri}	$-$	0.01099	11.5599
D	$-$	-1050.97	

Table 36 – 2-phase natural circulation characteristic time ratio parameters for helical SGs calculated at an average temperature of 271.05 ºC and a pressure of 127.5 bars for the prototype, and an average temperature of 217.25 ºC and a pressure of 40 bars for the model

Parameter	Unit	Helical SG	
		Full scale prototype	Scaled-down model
h_{lg}	J/kg	1.598 $(10)^6$	2.800 $(10)^6$
α	$-$	5%	5%
$\Delta\rho$	kg/m^3	699.88	824.91
u_f	m/s	5.0269	0.2064
a_c	m^2	1.622	0.0491
q_c	J/s	160 $(10)^6$	$(10)^6$
Π_h	$-$	2.7076	1.1117
D	$-$	0.58939	

5 DISCUSSION AND CONCLUSIONS

The results from the scaling-down section has two parts to discuss those are: the parameters of interest which provides the scaling-down ratios and the generated distortions. The proposed dimensions and scaling ratios for the vertical, horizontal, and helical SGs are listed in Table 37, Table 38 and Table 39 respectively. The scaling ratios were taken from model to prototype.

Table 37 – Proposed specifications for vertical SG model with corresponding scaling ratios

Parameter		**Value**		**Scaling ratio**
		Prototype	**Model**	
Thermal Power (at 1% power)		$43\ (10)^6\ W$	$(10)^6\ W$	1:43
Mass flow rate (total, primary)		$1198.23\ kg/s$	$13.48\ kg/s$	1:88.89
Mass flow rate (total, secondary)		$24.552\ kg/s$	$0.399\ kg/s$	1:61.45
Number of SGs		4	2	1: 2
Primary side pressure		$155\ Bars$	$40\ Bars$	1:3.875
Secondary side pressure		$90\ Bars$	$25\ Bars$	1:3.6
Cold leg temperature (primary)		303.35 ℃	224 ℃	-
Hot leg temperature (primary)		329 ℃	240 ℃	-
Feedwater temperature		230 ℃	70 ℃	-
Live steam temperature		303.35 ℃	224 ℃	-
SG dimensions	Height	$15.0\ m$	$3.75\ m$	1:4
	Diameter (outer)	$3.0\ m$	$0.8\ m$	1:4
SG tubes distribution	Layout	Triangular	Triangular	-
	Pitch	$27.43\ mm$	$27.43\ mm$	1:1
SG tubes specifications	Number	$5980\ tubes$	$222\ tubes$	1:26.94
	Diameter	$19.05\ mm$	$19.05\ mm$	1:1
	Thickness	$1.09\ mm$	$1.09\ mm$	1:1
	Length (average)	$25.0\ m$	$6.948\ m$	1:3.6

Table 38 – Proposed specifications for horizontal SG model with corresponding scaling ratios

Parameter		**Value**		**Scaling ratio**
		Prototype	**Model**	
Thermal Power (at 1% power)		$32\ (10)^6\ W$	$(10)^6\ W$	1:32
Mass flow rate (total, primary)		$1007.0\ kg/s$	$13.49\ kg/s$	1:74.65
Mass flow rate (total, secondary)		$17.935\ kg/s$	$0.399\ kg/s$	1:44.95
Number of SGs		4	2	1: 2
Primary side pressure		$162\ Bars$	$40\ Bars$	1:4.05
Secondary side pressure		$78\ Bars$	$25\ Bars$	1:3.12
Cold leg temperature (primary)		293.25 ℃	224 ℃	-
Hot leg temperature (primary)		328.9 ℃	240 ℃	-
Feedwater temperature		227 ℃	70 ℃	-
Live steam temperature		293.25 ℃	224 ℃	-
SG dimensions	Length	$13.82\ m$	$3.455\ m$	1:4
	Diameter (inner)	$4.2\ m$	$2.1\ m$	1:2
SG tubes distribution	Layout	Rectangular	Rectangular	-
	Pitch [mm]	22×24	22×72	1:1 & 1:0.333
SG tubes specifications	Number	$10978\ tubes$	$350\ tubes$	1:31.37
	Diameter	$16.0\ mm$	$16.0\ mm$	1:1
	Thickness	$1.5\ mm$	$1.5\ mm$	1:1
	Length (average)	$13.82\ m$	$3.455\ m$	1:2

From Table 37 and Table 38, all the parameters got shrunk from the scaling except the pitch between the tubes in the horizontal SG got increased. The pitch increase provides better spacing between the tubes to take advantage of the available space inside the SG. The parameters in both tables conserve the 1-phase natural circulation mass flow rate (equation 9), and the horizontal SG model additionally conserves the factor of characteristic pressure difference (equation 17). Consequently, the resulted mass flow rates for the desired 1 MW thermal heating power in the models provides 16 ℃ temperature difference between the hot leg and the cold leg for both the vertical and horizontal SG models.

Table 39 – Proposed specifications for helical SG model with corresponding scaling ratios

Parameter	Value		Scaling ratio
	Prototype	**Model**	
Thermal Power	160 $(10)^6$ W	$(10)^6$ W	1:160
Mass flow rate (total, primary)	1256.15 kg/s	8.56 kg/s	1:146.75
Mass flow rate (total, secondary)	75.71 kg/s	0.46 kg/s	1:164.59
Primary side pressure	127.5 $Bars$	40 $Bars$	1:3.188
Secondary side pressure	34.5 $Bars$	15 $Bars$	1:2.3
Cold leg temperature (primary)	258.3 ℃	204.5 ℃	-
Hot leg temperature (primary)	283.8 ℃	230 ℃	-
Feedwater temperature	204 ℃	160 ℃	-
Live steam temperature	301.67 ℃	228.3 ℃	-
Superheating temperature	57 ℃	30 ℃	-

One interesting finding is the absence of the helical SG's tubes information from Table 39. This is due to the fact that the tubes reside on another flow channel than the flow channel used in the calculation. Based on the calculated flow channel diameter (0.25 m), the parameters of interest could be dimensioned. The dimensioning includes 2 helical coils, one is coiled clock wise and the other coiled counter clock wise, tubes diameter, pitch between the tubes, and the total height the coils extends within as shown in Table 40. A schematic figure of the configuration is shown in Figure 17.

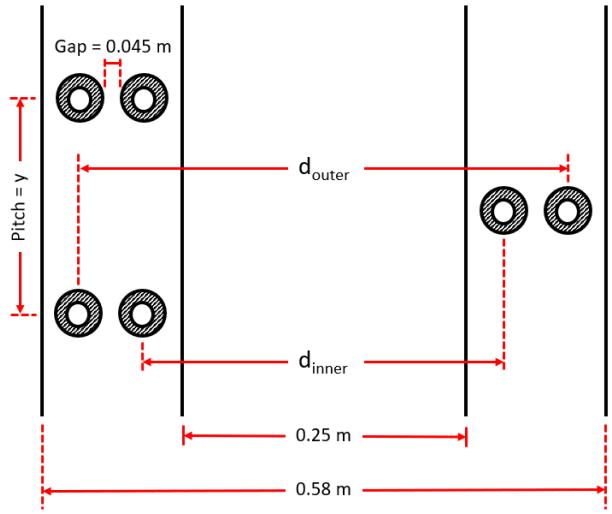

Figure 17 – Cross section of the proposed helical SG showing the 2 helical coil tubes and dimensions

Table 40 – Proposed dimensions for helical SG model

Parameter	Unit	Value
Flow channel height	m	1.30
Flow channel inner diameter	m	0.250
Flow channel outer diameter	m	0.580
Pitch for one complete tube turn	mm	22.5
Number of turns (height/pitch)	$-$	58
Tube diameter (outer diameter)	mm	15
Diameter of inner tube's circle (d_{inner})	m	0.355
Diameter of outer tube's circle (d_{outer})	m	0.475
Inner tube's length	m	64.70
Outer tube's length	m	86.56

Table 41 – Distortion for the scaled-down SGs

Distortion	Vertical SG	Horizontal SG	Helical SG
1-phase natural circulation	0.36986	0.62129	-1050.97
2-phase natural circulation	-0.96657	-0.85416	0.58939

The last concern to address from the scaling is the generated distortion. The distortion values for the three SG designs are listed in Table 41. The vertical and horizontal SG models show a very small distortion value for the 1-phase natural circulation characteristic time ratio which is likely due to the conservation of the mass flow rate in 1-phase steady state natural circulation as according to equation 9. Apparently, distortion for the 1-phase natural circulation was generated for the helical SG model because equation 9 was not used to conserve the mass flow rate. On the other hand, the 2-phase natural circulation characteristic time ratio for all the SG models had small distortion.

6 SUMMARY

The objective of this work was to understand the design of industrial steam generator of a vertical, horizontal, and helical layout and scale them down. The vertical steam generator is in the European Pressurized Reactor (EPR) which has 4 primary side loops and produces 4300 MW thermal. The horizontal steam generator is in the Russian AES-2006 which also has 4 primary side loops and produces 3200 MW thermal. The helical steam generator is in the modular NuScale reactor which has 2 steam generators and produces 160 MW thermal. These specific steam generators were chosen because they are the light water reactor designs of interest to LUT for the MOTEL test facility.

Available scaling methods were the power-to-volume which conserves the height and the heat flux, Ishii three-level scaling which is not limited by height conservation, H2TS which is practical and technically justifiable, and the FSA which is an advanced version of the H2TS method. Due to the practical nature of the H2TS it was chosen as the scaling method for all the 3 steam generator designs.

Using the H2TS method required the establishment of a hierarchy for the steam generators by breaking them down into smaller components. The desired phenomena to scale from the hierarchy was the 1-phase and 2-phase natural circulation. After the scaling of both phenomena, the scaling distortion was calculated.

Results from the scaling were used to make a proposal for the three SG models. The proposed designs include the size of the SG, operating pressure and temperatures, mass flow rates, tube sizes and layout, number of tubes, tube lengths, and tube diameters. Because the results for the helical SG from the scaling did not provide actual dimensions for the tubes, the dimensioning for them was done separately.

REFERENCES

1. Areva, 2005. *EPR,* Paris: Areva.
2. Bergman, T., Mirsky, S., Pope, S. & Unikewicz, S., 2016. *The NuScale Design,* Corvallis: NuScale Power.
3. D'Auria, F., 2017. *Thermal Hydraulics in Water-Cooled Nuclear Reactors.* 1st ed. s.l.:Woodhead Publishing.
4. D'Auria, F. & Galassi, G. M., 2010. *Scaling in Nuclear Reactor System Thermal-Hydraulics,* Pisa: Università di Pisa.
5. Dolganov, K. S. & Shishov, A. V., 2012. *Cross-verification of one- and three-dimensional models for VVER steam generator,* Mosco: Nuclear Safety Institute of the Russian Academy of Science (IBRAE RAS).
6. Hewitt, G. F. & Collier, J. G., 2000. *Introduction to Nuclear Power.* 2nd ed. s.l.:CRC Press.
7. Hyvärinen, J., Telkkä, J., Kauppinen, O.-P. & Purhonen, H., 2017. MOTEL - Modular design and physical principles of the next generation thermal hydraulics test facility at LUT. *17th International Topical Meeting on Nucear Reactor Thermal Hydraulics (NURETH-17),* Volume 9, pp. 5128-5141.
8. IAEA, 1974. *Thermal Discharges at Nuclear Power Stations Their management and environmental impacts,* Vienna: IAEA.
9. IAEA, 2007. *Nuclear Power Plant Design: Structure of Nuclear Power Plant Design Characteristics in the AEA Power Reactor Information System (PRIS),* Vienna: International Atomic Energy Agency.
10. IAEA, 2011. *Status report 108 - VVER-1200 (V-491),* Vienna: IAEA.
11. IAEA, 2014. *Updated Status On Global SMR Development.* [Online] Available at: https://www.iaea.org/NuclearPower/Downloadable/SMR/files/4_UPDATED_STATUS_ON_GLOBAL_SMR_DEVELOPMENT__as_of_September_2014.pdf [Accessed 04 July 2018].
12. IAEA, 2016. *Research Reactors: Purpose and Future,* Vienna: IAEA.
13. Incropera, F., Dewitt, D., Bergman, T. & Lavine, A., 2006. *Fundamentals of Heat and Mass Transfer.* 6th edition ed. Hoboken: John Wiley & Sons.

14. Ishii, M. et al., 1998. The three-level scaling approach with application to the Purdue University Multi-Dimensional Integral Test Assembly (PUMA). *Nuclear Engineering and Design,* Volume 186, pp. 177-211.
15. Kouhia, V. et al., 2014. *General description of the PWR PACTEL test facility - third edition,* Lappeenranta: Lappeenranta University of Technology.
16. Modro, S. M. et al., 2003. *Multi-Application Small Light Water Reactor Final Report,* Idaho Falls: Idaho National Engineering and Environmental Laboratory.
17. Nuclear Energy Agency, 2017. *A state-of-the-art report on scaling in system thermal-hydraulics applications to nuclear reactor safety and design,* Paris: Nuclear Energy Agency.
18. Nuclear Energy, 2018. *Nuclear Power Plant - What is it?.* [Online] Available at: https://nuclear-energy.net/definitions/nuclear-power-plant.html [Accessed 10 May 2018].
19. NuScale Power, 2018. *NuScale Standard Plant Design Certification Application - Chapter Four: Reactor,* Corvallis: NuScale Power.
20. NuScale Power, 2018. *NuScale Standard Plant Design Certification Application - Chapter One: Introduction and General Description of the Plant,* Corvallis: NuScale Power.
21. NuScale Power, 2018. *NuScale Standard Plant Design Certification Application - Chapter Ten: Steam and Power Conversion System,* Corvallis: NuScale Power.
22. Reuters, 2017. *Finland's Olkiluoto 3 reactor start delayed to May 2019.* [Online] Available at: https://www.reuters.com/article/finland-nuclear-olkiluoto/finlands-olkiluoto-3-reactor-start-delayed-to-may-2019-idUSL8N1MK13B [Accessed 29 May 2018].
23. Reyes, J. N., 2009. *Innovative Water-cooled Reactor Concepts - SMR,* Vienna: NuScale Power.
24. Reyes, J. N. & Hochreiter, L., 1998. Scaling analysis for the OSU AP600 test facility (APEX). *Nuclear Engineering and Design,* 53(109), pp. 53-109.
25. Riznic, J., 2017. *Steam Generators for Nuclear Power Plants.* 1st ed. s.l.:Woodhead Publishing.
26. Rosatom Overseas JSC, 2015. *The VVER today,* Moscow: Rosatom Overseas JSC.

27. Rosatom, 2018. *Projects.* [Online]
Available at: http://www.rosatom.ru/en/investors/projects/
[Accessed 15 June 2018].
28. Tuunanen, j. et al., 1998. *General Description of the PACTEL test facility,* Espoo: VTT Energy.
29. TVO, 2010. *Nuclear Power Plant Unit Olkiluoto 3,* Eurajoki: TVO.
30. TVO, 2018. *TVO confirms a settlement agreement signed on OL3 EPR project completion and related disputes.* [Online]
Available at: https://www.tvo.fi/news/1966
[Accessed 29 May 2018].
31. VTT, 2015. *Decommissioning of FiR 1 nuclear reactor.* [Online]
Available at: https://www.vttresearch.com/services/low-carbon-energy/nuclear-energy/decommissioning-of-finlands-first-nuclear-reactor
[Accessed 23 May 2018].
32. Westinghouse Electric Corporation, 1984. *The Westinghouse Pressurized Water Ractor Nuclear Power Plant.* s.l.:Water Reactor Divisions.
33. Zuber, N., 2001. The effects of complexity, of simplicity and of scaling in thermal-hydraulics. *Nuclear Engineering and Design,* Volume 204, pp. 1-27.
34. Zuber, N. et al., 1998. An integrated structure and scaling methodology for sever accident technical issue resolution: Development of methodology. *Nuclear Engineering and Design,* Volume 186, pp. 1-21.

APPENDIX 1. Estimating the total loss coefficient *F* for vertical and horizontal SGs

The calculation parameters in Table 42 and Table 43 were used to estimate the total loss coefficient *F* found in equation 9 for the vertical and horizontal SGs respectively. The values were chosen from the nominal operation of their respective reactors and were used in equation 13.

Table 42 – Estimation of total loss coefficient in EPR vertical SG at nominal operation (155 bars)

Parameter	Symbol	Unit	Value
Thermal Power	q_c	MW	4300
Density in cold leg (at $T_{CL} = 296$ ℃)	ρ_{CL}	kg/m^3	734.61
Density in hot leg (at $T_{HL} = 329$ ℃)	ρ_{HL}	kg/m^3	654.64
Density difference between cold and hot legs	$\Delta\rho$	kg/m^3	79.97
Average density in the primary side	ρ_{avg}	kg/m^3	694.625
Mass flow rate (primary side)	$\dot{m}$	kg/s	21085
Gravity constant	g	m/s^2	9.81
Pump head	H_{pump}	m	100.2
Total loss coefficient	F	$1/kg.m$	0.0015358

Table 43 - Estimation of total loss coefficient in AES-2006 horizontal SG at nominal operation (162 bars)

Parameter	Symbol	Unit	Value
Thermal Power	q_c	MW	3200
Density in cold leg (at $T_{CL} = 298.2$ ℃)	ρ_{CL}	kg/m^3	731.48
Density in hot leg (at $T_{HL} = 328.9$ ℃)	ρ_{HL}	kg/m^3	657.45
Density difference between cold and hot legs	$\Delta\rho$	kg/m^3	74.03
Average density in the primary side	ρ_{avg}	kg/m^3	694.465
Mass flow rate per SG (primary side)	$\dot{m}$	kg/s	17880
Gravity constant	g	m/s^2	9.81
Pump head	H_{pump}	m	62.2
Total loss coefficient	F	$1/kg.m$	0.001324

APPENDIX 2. Tubes distribution in horizontal SG (AES-2006)

The Horizontal SG model PGV-1000MKP which is used in AES-2006 reactor has 2 different arrays of tubes (inner pack and outer pack). Each array comes from both the front and back of the hot collector and are connected to the cold collector which gives a total of 4 array of tubes as shown in Figure 18. A cross-sectional view of the SG is shown in Figure 19.

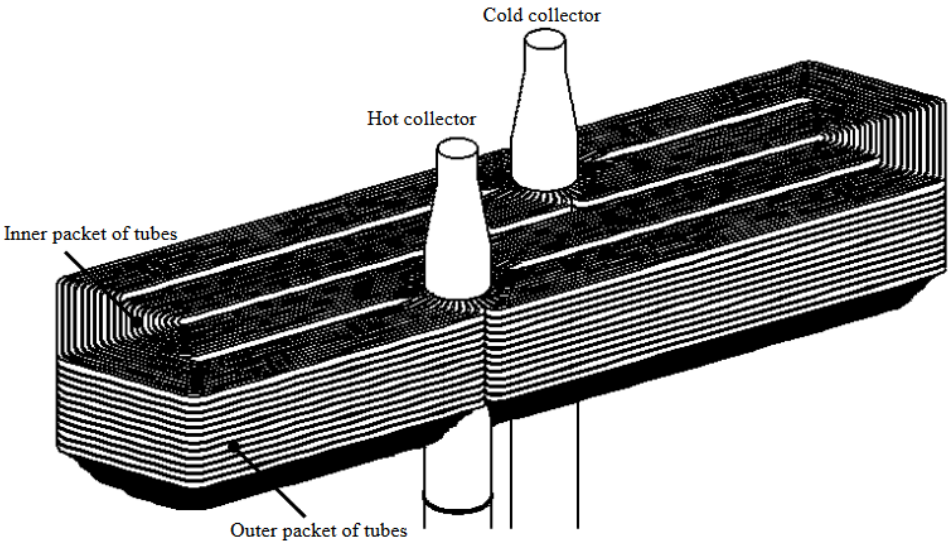

Figure 18 – Tube arrays in the PGV-1000MKP horizontal SG (Dolganov & Shishov, 2012, p. 6)

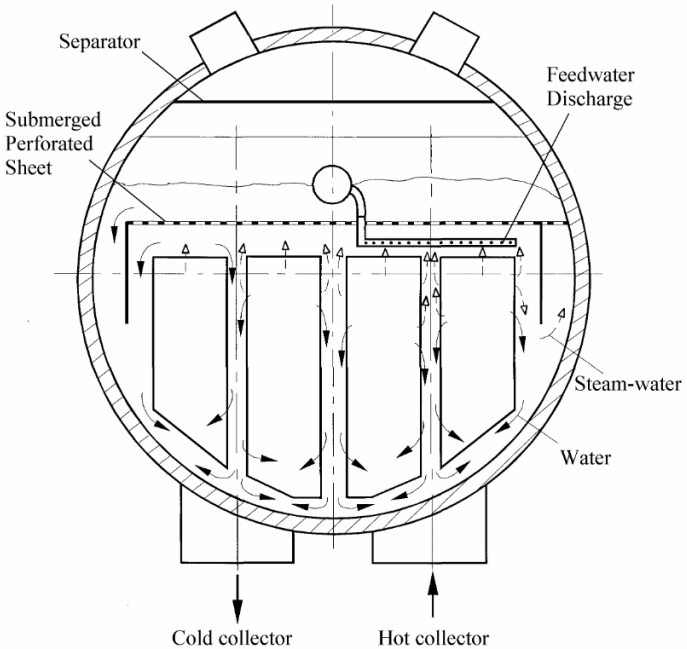

Figure 19 – Cross-section view of PGV-1000MKP Horizontal SG (Dolganov & Shishov, 2012, p. 4)

(continues)

APPENDIX 2. (continues)

Totally, there are 10978 tubes. The number of tubes in each array and the dimensions inside the SG were estimated according to the following assumptions:

1. The inner packet of tubes will be assumed to have 60% of the total tubes, and the remaining 40% will be on the outer packet of tubes.
    - Inner packet: 60% of tubes = 6588 tubes
    - Outer packet: 40% of tubes = 4390 tubes
2. The front side of the hot and cold collectors will hold half the amount of the tubes, and the back side of the collectors will hold the remaining half.
    - Inner packet tubes per one side = 3294 tubes
    - Outer packet tubes per one side = 2195 tubes
3. The tubes are distributed in a rectangular arrangement in each packet with the remaining tubes going in the bottom.
    - Inner packet tubes arrangement: (34×96) + 30 tubes in the bottom
    - Outer packet tubes arrangement: (34×64) + 19 tubes in the bottom
4. Using $22mm\times24mm$ pitch, the rectangular area the tubes cover in each tubes packet are calculated.
    - Inner packet size: $748mm\times2304mm$
    - Outer packet size: $748mm\times1536mm$
5. The other dimensions inside the SG are assumed as shown in Figure 20.

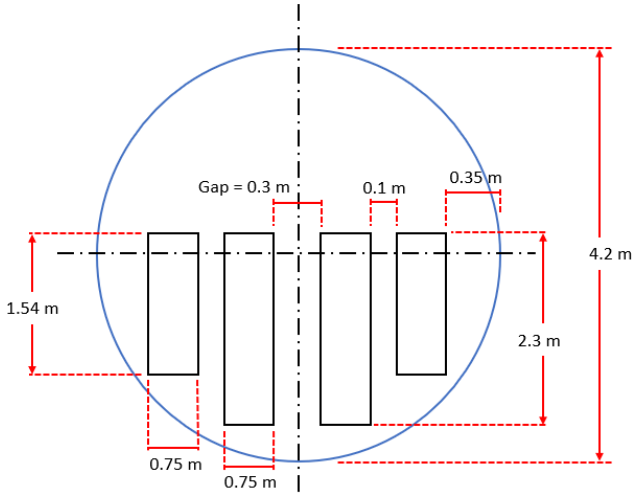

Figure 20 – Estimated dimensions for the PGV-1000MKP horizontal SG (figure is not to scale)

(continues)

APPENDIX 2. (continues)

6. The flow channel area between the pipes shown in Figure 21 is calculated as follows:

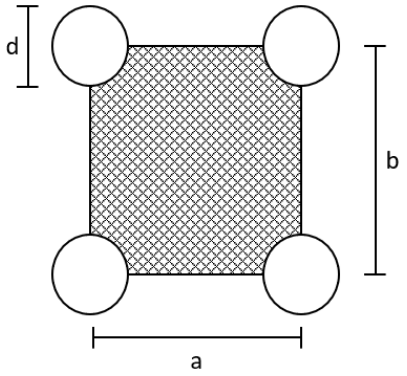

Figure 21 – Flow channel area between pipes in horizontal SG layout

$$Flow\ area = Rectangle\ area - \ one\ tube's cross\ section\ area$$
$$= (a)(b) - \frac{\pi}{4}\, d^2$$
$$= (0.022m)(0.024m) - \frac{\pi}{4}\,(0.016\,m)^2$$
$$= 0.000327\ m^2$$

7. Applying steps 1 to 6 for the scaled-down model gives the results below:

Total amount of tubes in inner and outer packets (totally 350 tubes)

- Inner packet: 60% of tubes = 210 tubes
- Outer packet: 40% of tubes = 140 tubes

Tubes amount in 1 side of a collector

- Inner packet tubes per one side = 105 tubes
- Outer packet tubes per one side = 70 tubes

Tubes distribution in rectangular arrangement

- Inner packet tubes arrangement: (9×11) tubes + 6 tubes in the bottom
- Outer packet tubes arrangement: (9×7) tubes + 7 tubes in the bottom

The area the tubes cover using $22mm \times 72mm$ pitch

- Inner packet size: $198mm \times 864mm$
- Outer packet size: $198mm \times 576mm$

Flow channel area using $22mm \times 72mm$ rectangular pitch

- Flow area = 0.00138 m^2